Atmospheric Environment 314 (2023) 120109

Contents lists available at ScienceDirect

Atmospheric Environment

journal homepage: www.elsevier.com/locate/atmosenv

Study of atmospheric glyoxal using multiple axis differential optical spectroscopy (MAX-DOAS) in India

Mriganka Sekhar Biswas [a,b], Prithviraj Mali [a,b], Christophe Lerot [c], Isabelle De Smedt [c], Anoop S. Mahajan [a,*]

[a] Indian Institute of Tropical Meteorology, Ministry of Earth Sciences, Pune, India
[b] Savitribai Phule Pune University, Pune, India
[c] Atmospheric Reactive Gases, Royal Belgian Institute for Space Aeronomy (BIRA-IASB), Brussels, Belgium

HIGHLIGHTS

- MAX-DOAS observations of atmospheric CHOCHO reported from three locations in India (Pune, Mahabaleshwar and Delhi).
- The Highest average CHOCHO vertical column densities (VCDs) and volume mixing ratios (vmr) were observed over urban Delhi.
- The lowest VCD and vmr were observed at the forested rural location of Mahabaleshwar.
- Higher/lower average VCDs were found during winter/pre-monsoon over urban Pune.
- Comparison with TROPOMI satellite retrievals showed an underestimation of atmospheric CHOCHO by TROPOMI.

GRAPHICAL ABSTRACT

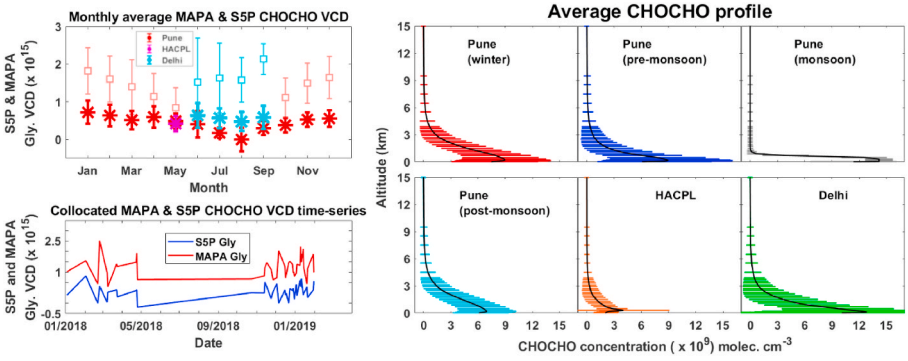

ARTICLE INFO

Keywords:
Glyoxal (CHOCHO)
MAX-DOAS
Satellite validation

ABSTRACT

Glyoxal (CHOCHO) is an important atmospheric trace gas formed by the oxidation of volatile organic compounds (VOCs). We present a study of atmospheric CHOCHO from three locations (Pune, Mahabaleshwar and Delhi) in India using Multi-Axis Differential Optical Spectroscopy (MAX-DOAS) observations. Pune and Delhi represent urban environments, whereas Mahabaleshwar represents a forested rural region. Differential slant column densities (dSCDs), vertical column densities (VCDs), surface volume mixing ratios (vmr) and vertical profiles of CHOCHO were measured and compared to satellite observations. Delhi showed the highest average CHOCHO VCD ($1.57 \pm 0.98 \times 10^{15}$ molec. cm^{-2}) and vmr (average of 0.43 ± 0.27 ppb), whereas Mahabaleshwar showed the lowest average VCD ($0.66 \pm 0.40 \times 10^{15}$ molec. cm^{-2}) and average vmr (0.08 ± 0.03 ppb) among the three sites. Average CHOCHO VCD ($1.52 \pm 0.66 \times 10^{15}$ molec. cm^{-2}) and vmr (0.33 ± 0.18 ppb) over Pune were close to but lower than Delhi. A large seasonal variation was observed in Pune, with the highest ($1.82 \pm 0.62 \times 10^{15}$ molec. cm^{-2}) and lowest ($0.79 \pm 0.45 \times 10^{15}$ molec. cm^{-2}) monthly average VCDs observed in January and May, respectively. This inter-annual pattern was observed in both ground-based and satellite observations. Satellite observations systematically underestimated the CHOCHO VCDs compared to ground-based

* Corresponding author.
E-mail address: anoop@tropmet.res.in (A.S. Mahajan).

https://doi.org/10.1016/j.atmosenv.2023.120109
Received 26 May 2023; Received in revised form 12 September 2023; Accepted 22 September 2023
Available online 24 September 2023

observations. Comparison with previous studies shows that Pune and Delhi have similar levels of CHOCHO with respect to other urban regions, while Mahabaleshwar is comparable to other remote environments worldwide.

1. Introduction

Glyoxal (CHOCHO) is one of the most abundant dicarbonyl compounds in the troposphere (Volkamer et al., 2005a; Vrekoussis et al., 2009). It is a crucial intermediate of atmospheric ozone formation and results from the oxidation of various volatile organic compounds (VOCs) (Myriokefalitakis et al., 2008; Seinfeld and Pandis, 2016). Oxidation of VOCs (with two carbons or higher) contributes more towards atmospheric CHOCHO than primary emissions (Fu et al., 2008). Globally, oxidation of biogenic VOCs accounts for the most significant contribution (55%) of tropospheric CHOCHO, followed by biomass burning (20%), biofuel (17%), and anthropogenic emissions (8%), respectively (Fu et al., 2008). Enhanced CHOCHO concentrations coincide with biogenic and anthropogenic emission hotspots (Alvarado et al., 2014; Lerot et al., 2021; Seinfeld and Pandis, 2016). Isoprene and monoterpenes are the main biogenic precursors, whereas acetylene is the main anthropogenic precursor (Fu et al., 2008 and references therein). Isoprene oxidation accounts for 65–70% of all atmospheric CHOCHO (Fu et al., 2008; Seinfeld and Pandis, 2016; Wennberg et al., 2018). The second-largest contributor of atmospheric CHOCHO is acetylene, accounting for 20% of all CHOCHO, and is more important in urban environments (Fu et al., 2008). Biogenic emissions of VOCs are affected by humidity, temperature, humidity and plant type (Guenther et al., 2000; Seinfeld and Pandis, 2016), and thus CHOCHO concentrations also depend on these parameters.

Photolytic decomposition is the primary sink for atmospheric CHOCHO (Seinfeld and Pandis, 2016; Tadić et al., 2006). Oxidation by hydroxyl (OH) radicals is another vital pathway for atmospheric CHOCHO removal (Seinfeld and Pandis, 2016; Setokuchi, 2011). Secondary organic aerosol (SOA) formation, oxidation by nitrate (NO_3), dry and wet depositions are other significant removal pathways (Fu et al., 2008; Seinfeld and Pandis, 2016; Volkamer et al., 2007). Due to these multiple removal processes, the average global lifetime of atmospheric CHOCHO is less than 4 h and in the tropics, it can be as low as 1–2 h (Fu et al., 2008, 2019; Myriokefalitakis et al., 2008; Volkamer et al., 2005a).

Remote sensing of atmospheric CHOCHO is possible due to its photosensitivity. Differential Optical Absorption Spectroscopy (DOAS) (Plane and Saiz-Lopez, 2006; Platt and Stutz, 2008) based observations from ground-based (Li et al., 2013; MacDonald et al., 2012; Mahajan et al., 2014; Volkamer et al., 2005a), airborne (Kluge et al., 2020), and satellite-borne (Alvarado et al., 2020; Wittrock et al., 2006) instruments have been reported from different environments around the world. Volkamer et al. (2005a) reported the first direct observation of atmospheric CHOCHO using the DOAS technique from Mexico City. Wittrock et al. (2006) reported the first global observation of CHOCHO using the Scanning Imaging Absorption Spectrometer for Atmospheric Cartography (SCIAMACHY) satellite. Various studies have reported higher CHOCHO columns over forested regions like in the Amazon (Wittrock et al., 2006) and in Borneo (MacDonald et al., 2012), over regions with high population density like China and India (Lerot et al., 2021; Wittrock et al., 2006) and over regions with high biomass burning (Alvarado et al., 2020; Kluge et al., 2020). Although the first DOAS-based CHOCHO observations were done more than a decade ago, there are scant ground-based observations of CHOCHO in India. Hoque et al. (2018b) reported the first MAX-DOAS observation of CHOCHO from India at Pantnagar. Later, Lerot et al. (2021) compared TROPOMI satellite-measured CHOCHO with MAX-DOAS observations from Pantnagar and Mohali in India.

Considering that studies of atmospheric CHOCHO are essential for understanding atmospheric VOC chemistry and the overall oxidative capacity of the troposphere, here we present CHOCHO observations from three different locations in India, representing three different environments. We study the seasonal and diurnal variation of atmospheric CHOCHO, and the vertical distribution of CHOCHO and compare the vertical columns with satellite observations.

2. Observation details

2.1. Site description

MAX-DOAS observations were conducted at three different locations in India. The first location is the Prithvi hostel in Pune City. Pune is India's 8th most populous city (Office of the Registrar General & Census Commissioner, India, 2011) in western India with an elevation of 560 m above sea level (asl). This location represents observation from an urban environment. There are various industrial establishments (in the northeast and northwest) and commercial, residential settlements (in the east, southeast and south) within a ~12 km radius of the observation site. The MAX-DOAS scanner was pointed at a 355° azimuth angle to the north overlooking an academic institute and was installed at ~30 m above ground (~590 m asl). The year-long observation spanned from January 2, 2018 to February 8, 2019. However, there were three gaps in the MAX-DOAS observations (15th July–14th August 2018; 22nd August–10th September 2018; and 30th September–21st October 2018) due to cloudy conditions, instrumental and logistical issues (Biswas and Mahajan, 2021). There are four different seasons observed over Pune, pre-monsoon or summer (March–May), monsoon (June–September), post-monsoon (October–December), and winter (January–February). Further details of the Pune observation site are available in Biswas and Mahajan (2021). The second location is the 'High Altitude Cloud Physics Laboratory' (HACPL), at Mahabaleshwar, a hill station (1378 m asl) in India's Western Ghats Mountain range. The observation at Mahabaleshwar was conducted during the pre-monsoon period, from April 25 to May 30, 2018. As part of the Western Ghats with dense vegetative cover, Mahabaleshwar represents a forested rural environment which rises above the boundary layer during the night and early mornings. The HACPL is situated on a mountain plateau covered with dense vegetation with an elevation of ~800 m from the mountain base. The plateau stretches ~4–6 km surrounding the HACPL site. There are two towns in the east at ~9 km (Panchgani) and ~15 km (Wai) distance. There are a few villages within ~25 km from the HACPL site. The MAX-DOAS scanner was pointed towards the north, overlooking the forest canopy at ~10 (~1388 m asl) m above ground. Further details of the observation site are available in Biswas et al. (2021). The third location is the Indian Institute of Tropical Meteorology, Delhi (IITM, Delhi) campus (28.630° N, 77.175° E) in New Delhi with an elevation of 216 m asl. New Delhi is one of the most polluted cities in the world (Chowdhury et al., 2017; WHO, 2016) and is located in the Indo-Gangetic Plain (IGP) with a high population density (Singh et al., 2015). The IITM Delhi location represents an urban environment with high traffic density (Tiwari et al., 2015). The instrument scanner was pointed at 240° azimuth angle to the north at ~10 m (~226 asl) above ground. MAX-DOAS observations in Delhi were carried out from June 3 to September 16, 2019, during the monsoon season. Fig. 1 shows the observation locations. Table 1 presents key details regarding the observation sites.

2.2. MAX-DOAS measurement details

The MAX-DOAS technique involves the measurement of scattered background solar radiation at different elevation angles with respect to the instrument's position (Hönninger et al., 2004). Observations at different elevation angles provide information about trace gas

concentration from different layers in the atmosphere. Two different MAX-DOAS instruments were used in the three campaigns. Both the spectrometers are of the same make with the same components. The algorithms used to analyse the MAX-DOAS observations are the same. Both the MAX-DOAS instruments have two parts, scanner and spectrometer units. The outdoor scanner unit directs the scattered solar radiation towards the indoor spectrometer. The field of view of the scanner is 0.2°. The scanner unit is mounted on a high location (e.g., the rooftop of a building) with a clear line of sight on the horizon. Two ultra-low stray light 75 mm Avantes spectrometers (one spectrometer for operating within UV spectral range, another for visible spectrum) with a full-width half maxima resolution of 0.7 nm and 100 μm slit are contained within the spectrometer unit. The instrument used in Pune and Delhi campaigns has an operating spectral range of 306.08–468.77 nm (UV spectrometer) and 441.91–583.36 nm (visible spectrometer). In comparison, the instrument used in Mahabaleshwar has a spectral range of 301.50–463.73 nm and 443.54–584.19 nm. Scattered solar radiation from 9 different elevation angles (1°, 2°, 3°, 5°, 10°, 20°, 40° and 90°) with respect to instrument position were recorded during the campaigns. The maximum exposure time for a single spectrum was limited by 70% saturation of the charged coupled device (CCD) sensor. For SZA less than 80°, the total exposure time per elevation angle was set to 60 s. The total exposure duration was set to 90 s for SZA 80°–90° and 120 s for SZA 90°–100°, respectively. The mercury calibration spectra, dark current and offset spectra and were recorded at the end of each day (when SZA> 100°). The spectra were calibrated during post-processing using the Fraunhofer spectrum (Kurucz et al., 1984), and mercury emission lines (recorded daily). In addition, dark current and offset were recorded for the respective MAX-DOAS instrument and removed from the spectra. After initial corrections from dark current and offset spectra, solar spectra were analyzed using QDOAS spectral fitting software (Danckaert et al., 2014; Fayt and Van Roozendael, 2013) (http://uv-vis.aeronomie.be/software/QDOAS/). The stratospheric contribution to the off-axis observations was eliminated using the zenith spectra from each scan cycle as a reference (Hönninger et al., 2004). For further details on the used instruments and measurement techniques, please refer to Biswas et al. (2021, 2019).

Apart from CHOCHO, the atmospheric pressure-induced oxygen dimer (O_4) was also analyzed using QDOAS. The wavelength window for O_4 differential slant column density (dSCD) retrieval was 351–390 nm. Table 2 contains the DOAS settings used for O_4 and CHOCHO retrievals. Several groups in the past have retrieved atmospheric CHOCHO at different wavelength intervals, as reported in Table 3. However, the community has no consensus regarding the correct wavelength interval for CHOCHO retrievals. We have tested three different wavelength windows (400–460 nm, 420–460 nm and 435–460 nm) and found that the retrieval using 435–460 nm window yields higher CHOCHO vertical column densities (VCDs) and surface volume mixing ratios (vmr) followed by 420–460 nm and 400–460 nm windows. We decided to use 435–460 nm windows as TROPOMI satellite retrievals were done in the same wavelength range (Lerot et al., 2021) and in the present study, we compare our ground-based CHOCHO retrievals with TROPOMI CHOCHO product. Examples of the DOAS fits for oxygen dimer (O_4), and CHOCHO are given in Fig. 2.

DOAS algorithms apply the Beer-Lambert law within a constrained wavelength range for the retrieval trace gas information. The logarithm of the ratio of the measured spectrum to the reference spectrum (e.g., a spectrum along the zenith viewing direction, where the light path through the trace gas layer is the shortest) is used to fit molecular absorption cross-sections. The dSCDs are retrieved from the resulting fit coefficients. The corresponding contributions to the measured optical density are resolved using high-frequency spectrum structures of the various absorbing species. This is accomplished using a least-squares fitting method for the individual species. The sensitivity of the sum of squares (in the least square method) with regard to fluctuations of the fitted parameters around the minimum and the noise on the measurements determine the degree of uncertainty on the retrieved dSCDs. A statistical model is utilized to assess the error of the fitted parameters. The statistical model considers that the errors in the measurements are independent and regularly distributed for each frequency (Danckaert et al., 2014). The dSCD errors are then propagated in MAPA model to estimate VCD and mixing ratio errors. For further details on the CHOCHO retrieval error, please refer to Danckaert et al. (2014) and Beirle et al. (2019).

2.3. MAPA model description

The VCDs and vertical concentration profiles of CHOCHO were retrieved from the MAX-DOAS observed dSCDS by employing the Mainz profile algorithm (MAPA) (Beirle et al., 2019). This algorithm follows a two-step approach to obtain a trace gas vertical profile from MAX-DOAS observations. First, the aerosol extinction profile is retrieved from the O_4 dSCDs observations. In the next step, the retrieved aerosol profiles are used as input to retrieve CHOCHO profiles. Both steps here consist of the same approach: a forward model and an inversion algorithm (MAPA). The forward model is provided as a look-up table (LUT). The LUT is calculated offline with the Monte Carlo Atmospheric Radiative Transfer Inversion Model (McArtim) (v1) (Deutschmann et al., 2011). For a detailed discussion of the inversion technique of the MAPA algorithm, please refer to (Beirle et al., 2019).

Some previous studies have reported a significant mismatch between modelled and measured O_4 dSCDs, which can be corrected using a scaling factor (SF = 0.8) applied to the measured O_4 absorption (Beirle et al., 2019; Clémer et al., 2010; Kumar et al., 2020; Wagner et al., 2010, 2019). However, our recent study (Mali et al., under review) found that aerosol optical depth (AOD) values obtained using MAPA agreed with AERONET measurements even without using a scaling factor for O_4 (i.e., SF = 1.0). Furthermore, since the same retrieved aerosol profiles were

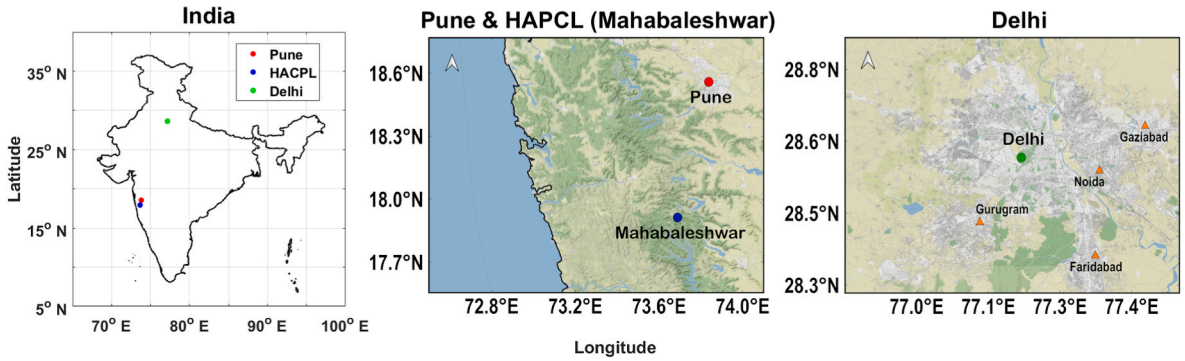

Fig. 1. Locations of the three observations sites across India. On the left, Pune city (red dot), HACPL, Mahabaleshwar (blue dot) and Delhi (green dot) are shown. The center and right panels show satellite images of Pune, Mahabaleshwar and Delhi.

used in this study to obtain CHOCHO profiles, no scaling factor was applied in the CHOCHO retrievals either. Similar to our study, few studies in the past have also concluded that there is no requirement for a scaling factor to attain consistency between the measured and modelled O_4 dSCDs (Ortega et al., 2016; Peters et al., 2012; Schreier et al., 2015). MAPA generates various profile parameters as output to ascertain the quality of the profile retrievals and identify valid dSCD sequences. The erroneous results were then filtered using these profile parameters after passing through a quality check (Beirle et al., 2019).

2.4. TROPOMI observations of CHOCHO VCDs

Satellite observations of CHOCHO from The TROPOspheric Monitoring Instrument (TROPOMI) on board the Copernicus Sentinal-5 Precursor (S5P) satellite were used for comparison. This sun-synchronous satellite has an equatorial overpass time of 13:30 local time. The nadir-viewing instrument is dedicated to the measurement of atmospheric constituents. TROPOMI provides quasi-daily global coverage of various atmospheric trace gases at 3.5 × 7 km^2 (before August 2019) in the UV–visible spectral range. CHOCHO dSCDs were retrieved in 435–460 nm wavelength range, the same as the MAX-DOAS retrievals. For further details on the TROPOMI instrument and CHOCHO retrieval, please refer to Kleipool et al. (2018), Lerot et al. (2021) and Ludewig et al. (2020).

2.5. Ambient $PM_{2.5}$ and PM_{10} data over Delhi

Ambient $PM_{2.5}$ and PM_{10} data was compared with MAX-DOAS CHOCHO observations over Delhi for the day of 9th June 2019 (which showed high CHOCHO mixing ratio). The $PM_{2.5}$ and PM_{10} data were collected from a nearby observation site at Pusa (~2 km from the IITM-Delhi site) maintained by India Meteorological Department (IMD). The data was achieved by the Central Pollution Control Bureau (CPCB) under the Ministry of Environment, Forest and Climate Change (MoEFCC) of India. Data was downloaded from https://app.cpcbccr.com/ccr/#/caaqm-dashboard/caaqm-landing (last access: April 03, 2023 11:00:00 h IST). The data has a temporal resolution of 15 min. Details of the measurements are available in Schnell et al., 2018.

2.6. ERA5 mean surface downward short-wave radiation flux data over Pune

Surface downward short-wave radiation flux data from ERA5 reanalysis product (Hersbach et al., 2023; last accessed: August 30, 2023 06:00 h UTC) over Pune was compared with CHOCHO VCDs to identify the effect of photochemistry on atmospheric CHOCHO. The data has a horizontal resolution of 0.25° × 0.25° and a temporal resolution of 1 h. The hourly mean surface downward short-wave radiation flux data was averaged over 0.5° × 0.5° box over Pune. For further details on the data, please refer to Hersbach et al., 2023.

2.7. MAX-DOAS observation of nitrogen dioxide (NO_2) over Pune

MAX-DOAS observation of NO_2 over Pune was compared with CHOCHO observations to identify the effect of local emission on atmospheric CHOCHO. The NO_2 data were measured using the above-mentioned MAX-DOAS instruments. NO_2 dSCDs were retrieved in the 415–440 nm wavelength window. As discussed above, the NO_2 VCDs and mixing ratios were calculated using the MAPA model.

Table 2
DOAS analysis settings.

Parameters	O_4 (UV.)	CHOCHO	References
Fitting window	351–390 nm	435–460 nm	
Polynomial order	5th order	3rd order	
Orthobase order	2nd order	2nd order	
Linear offset	none	none	
Reference spectra	✓	✓	zenith spectra from scan cycle
O_4	✓	✓	293 K, Thalman and Volkamer (2013)
O_3	✓	✓(I_0 correction of 10^{20} molec. cm^{-2})	223 K, Serdyuchenko et al. (2014)
	✓	✓(I_0 correction of 10^{20} molec. cm^{-2})	243 K, Serdyuchenko et al. (2014) (orthogonalized to O_3 spectra at 223 K)
NO_2	✓	✓(I_0 correction of 10^{17} molec. cm^{-2})	294 K, Vandaele et al. (1998)
	✓	✓(I_0 correction of 10^{17} molec. cm^{-2})	220 K, Vandaele et al. (1998) (orthogonalized to NO_2 spectra at 294 K)
HCHO	✓		298 K, Meller and Moortgat (2000)
CHOCHO		✓	296 K, Volkamer et al. (2005b)
HONO	✓		298 K, Stutz et al. (2000)
BrO	✓		223 K, Fleischmann et al. (2004)
H_2O		✓(I_0 correction of 10^{24} molec. cm^{-2})	296 K, Rothman et al. (2010)
Ring spectra	✓	✓	Ring spectra, Chance and Kurucz (2010)

2.8. Aerosol optical depth (AOD) observations from AERONET network over Pune

Aerosol Robotic NETwork (AERONET) station in Pune (18.537° N, 73.805° E, ~595 AMSL) measures the AOD using CIMEL CE 318 sun photometer. Level 2 AOD products which passed a quality assurance and cloud-screen were compared with CHOCHO data. AERONET AOD data in Pune are available at 4 different wavelength (440 nm, 675 nm, 870 nm, and 1020 nm). For this study we have used AOD at 440 nm.

2.9. Back-trajectory analysis

Hybrid Single Particle Lagrangian Integrated Trajectory Model (HYSPLIT) was used to do back-trajectory analysis for air parcels that arrived at the observation station (Draxler and Hess, 1998). The HYSPLIT model was run with daily gridded meteorological data from the

Table 1
MAX-DOAS observation site details.

Location	Coordinates	Instrument elevation (above sea level)	Campaign period (season)	Environment type	Instrument azimuth angle (compared to geometric North)
Pune City	18.542° N, 73.804° E	~590 m	January 2, 2018 to February 8, 2019 (winter, pre-monsoon and post-monsoon)	Urban	355°
Mahabaleshwar	17.92° N, 73.65° E	~1388 m	25th April to 30th May 2018	Forested rural	0°
Delhi	28.630° N, 77.175° E	~226 m	3rd June to 16th September 2019 (monsoon)	Urban	240°

Table 3
CHOCHO comparison with previous studies.

Sr. No.	Authors	location	Environment type	period	technique	CHOCHO retrieval window	CHOCHO range	CHOCHO mean
1	Volkamer et al. (2005b)	Mexico city	Urban	31st March to May 4, 2003.	LP-DOAS	420–465 nm	<0.15–1.82 ppbv (mixing ratio)	
2	Sinreich et al. (2007)	MIT, Cambridge	Urban	1st July – August 15, 2004	MAX-DOAS	420–460 nm	40–140 pptv (mixing ratio)	
3a	Khokhar et al. (2016)	Mainz, Germany	Urban	18th June - July 17, 2013	MAX-DOAS	434–460 nm	Upto 1.4×10^{16} molec. cm^{-2} (VCDs)	
3b	Khokhar et al. (2016)	Islamabad, Pakistan	Urban	18th June - July 17, 2015	MAX-DOAS	434–460 nm	Upto 7.81×10^{15} molec. cm^{-2} (VCDs)	
4a	Gratsea et al. (2016)	Athens, Greece	Urban	October 2012 to March 2014	MAX-DOAS	434–458 nm		$(1.8 \pm 0.8) \times 10^{15}$ molec. cm^{-2} (dSCD)
4b	Gratsea et al. (2016)	Athens, Greece	Rural	October 2012 to March 2014	MAX-DOAS	434–458 nm		$(1.4 \pm 0.6) \times 10^{15}$ molec. cm^{-2} (dSCD)
5	Hoque et al. (2018a)	Pantnagar, India	semi-urban	January–November 2017	MAX-DOAS	436 − 457 nm		~0.2 ppb (during autumn)
6	Javed et al. (2019b)	Beijing, China	Urban	09th May – September 09, 2017	MAX-DOAS	438–457 nm	$(1.33–9.77) \times 10^{14}$ molec. cm^{-2} (VCDs)	
7a	Javed et al. (2019a)	Beijing, China	Urban	May 2017–April 2018	MAX-DOAS	438–457 nm	$(0.43–2.18) \times 10^{15}$ molec. cm^{-2} (VCDs)	
7b	Javed et al. (2019a)	Baoding, China	Urban	May 2017–April 2018	MAX-DOAS	438–457 nm	$(0.37–2.07) \times 10^{15}$ molec. cm^{-2} (VCDs)	
8	Benavent et al. (2019)	Madrid, Spain	Urban	2014–2016	MAX-DOAS	424–457 nm with a gap of 442–449 nm	0.7–2 ppb (monthly hourly average)	
9	Schreier et al. (2020)	Vienna, Austria	Semi-urban	2017–2018	MAX-DOAS	433–458 nm	~50–80 ppt (monthly average)	
10	Ryan et al. (2020)	Melbourne, Australia	Urban	December 2016–May 2019	MAX-DOAS	435–456.5 nm	$(1.17–4.65) \times 10^{14}$ molec. cm^{-2} (VCDs)	
11	Zhang et al. (2021)	Qingpu, Shanghai, China	Sub-urban	17th October - 21st November 2019	MAX-DOAS	400–460 nm		0.2 ± 0.1 ppbv (mixing ratio)
12	Guo et al. (2021)	Shanghai, China	urban	26th June - 9th August 2018	LP-DOAS	440–455 nm		0.164 ± 0.073 ppbv
13	Hoque et al. (2018a)	Phimai, Thailand	rural	October 2014–October 2016	MAX-DOAS	436–457 nm	~0.05–0.2 ppb	
14	Xing et al. (2020)	Changshou, China	rural	December 27, 2018–January 16, 2019	MAX-DOAS	431–460 nm	0.03–0.17 ppb	
15	MacDonald et al. (2012)	Borneo rainforest	Remote forest	April–July 2008	LP-DOAS	422–442 nm	Upto 1.6 ppb (typical range 0.8–1 ppb during day)	
16	Baidar et al. (2013)	California, USA	Air-borne observation	19 May – 19 July 2010	Airborne MAX-DOAS	433–460 nm		274 ± 28 pptv (mixing ratio within boundary layer)
17	Kluge et al. (2020)	Amazon basin	Air-borne observation	September–October 2014	mini-DOAS	420–465 (gap 439–447 nm)	85–250 ppt	
18	Present work	Pune city, India	Urban	January 2, 2018 - February 8, 2019	MAX-DOAS	435–460 nm	$(0.06–5.33) \times 10^{15}$ molec. cm^{-2} (VCD)	$(1.52 \pm 0.66) \times 10^{15}$ molec. cm^{-2} (VCD)
							0.02–2.12 ppb (vmr)	0.33 ± 0.18 ppb (vmr)
19	Present work	HACPL, Mahabaleshwar, India	Forested region	25th April – May 30, 2018	MAX-DOAS	435–460 nm	$(0.13–1.95) \times 10^{15}$ molec. cm^{-2} (VCD)	$(0.66 \pm 0.40) \times 10^{15}$ molec. cm^{-2} (VCD)
							0.01–0.19 ppb	0.08 ± 0.03 ppb
20	Present work	Delhi city, India	Urban	3rd June - September 16, 2019	MAX-DOAS	435–460 nm	$(0.06–4.87) \times 10^{15}$ molec. cm^{-2} (VCD)	$(1.62 \pm 0.98) \times 10^{15}$ molec. cm^{-2} (VCD)
							0.10–1.62 ppb (vmr)	0.43 ± 0.27 ppb (vmr)

Global Data Assimilation System (GDAS) with a resolution of 0.5° × 0.5°. Past 12 h back-trajectories of the air parcels arriving at the observation station were calculated every hour.

2.10. Fire data

The National Aeronautics and Space Administration (NASA) Earth observations repository was used to collect fire data from Moderate Resolution Imaging Spectroradiometer (MODIS) aboard Terra and Aqua satellites (NASA, 2020). The impact of pollutants transported from surrounding fire events to the observation location was investigated using daily gridded fire count data (MOD14A1) at a resolution of 0.1° × 0.1°. A downscaled spatial resolution of 0.5° × 0.5 was applied to the data. The "no fire" events were related to the grid points that did not display any fire counts. The median value of all the fire occurrences for each grid point across the Indian subcontinent was calculated. "High fire" events were associated with grid points if their fire counts exceeded the median value. "Low fire" incidents related to grid points having fire counts below the median value.

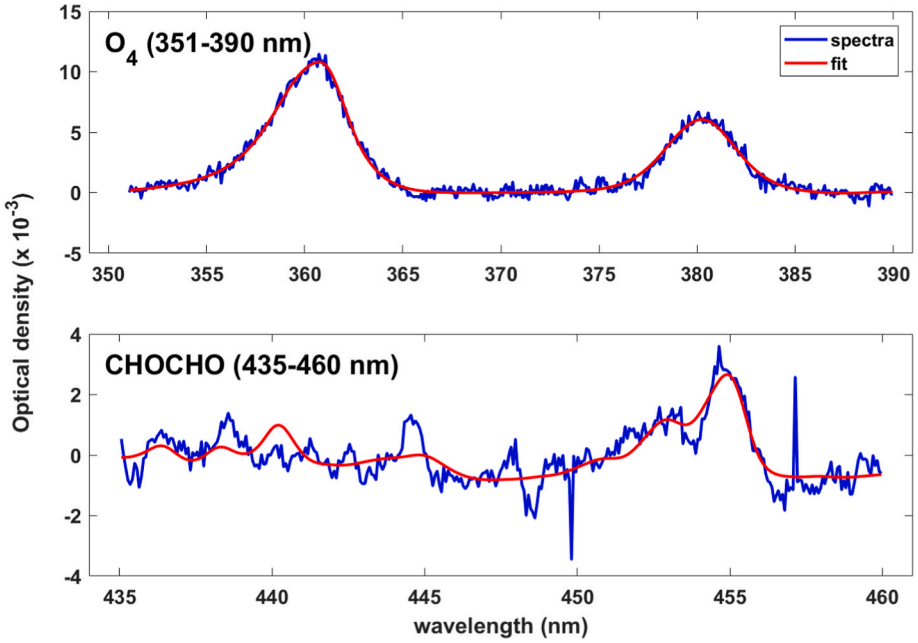

Fig. 2. DOAS fits for O_4 and CHOCHO. (Top panel) O_4 (351–390 nm): 20th April 2018 03:25 h (UTC); SZA: 52.9°; Elevation angle (EA): 3.0°; dSCD: $2.6 \times 10^{43} \pm 3 \times 10^{41}$ molecules^2 cm^{-5}; RMS: 4.2×10^{-4}. (Bottom panel) CHOCHO (435–460 nm): 13th April 2018 07:21 h; SZA: 10.28°; EA: 3.0°; dSCD: $7.45 \times 10^{15} \pm 4.4 \times 10^{14}$ molec. cm^{-2}; RMS: 5.6×10^{-4}.

3. Results

3.1. Differential slant column densities (dSCDs) from MAX-DOAS

The longest CHOCHO observations among the three sites were made at Pune, where the year-long measurements encompass four different seasons. The highest average dSCD values for all seasons were observed at 1° elevation angle. The annual average dSCD at 1° elevation angle is $1.84 \times 10^{15} \pm 0.62 \times 10^{15}$ molec. cm^{-2}. The maximum seasonal average was found during monsoon ($2.07 \times 10^{15} \pm 0.49 \times 10^{15}$ molec. cm^{-2}), and the minimum was observed during post-monsoon ($1.62 \times 10^{15} \pm 0.47 \times 10^{15}$ molec. cm^{-2}).

The highest (among three sites) average CHOCHO dSCD was observed at Delhi ($2.37 \pm 0.82 \times 10^{15}$ molec. cm^{-2}). CHOCHO at Delhi was even higher than the corresponding dSCDs over Pune during the monsoon season. The maximum CHOCHO dSCDs over Delhi was $6.16 \pm 0.51 \times 10^{15}$ molec. cm^{-2}. Mahabaleshwar had the lowest (among three sites) average CHOCHO dSCDs of $1.35 \pm 0.41 \times 10^{15}$ molec. cm^{-2} with a range of 0.57–2.78 $\times 10^{15}$ molec. cm^{-2}. Fig. 3 shows the time-series plots for CHOCHO dSCDs at the three locations.

3.2. Vertical column densities (VCDs) and volume mixing ratios (vmr)

Fig. 3 shows the time-series of CHOCHO VCDs and vmr from all three locations. Depending on various profile parameters generated by MAPA model, the VCDs and mixing ratios of CHOCHO were filtered. Some of these filtering parameters include proxies for cloud cover, unusually high AOD values, exceptionally high aerosol layer height, relatively higher dSCD errors compared to corresponding dSCDs etc. As mentioned earlier, there were gaps in the MAX-DOAS observations during the monsoon period in Pune. Most of the CHOCHO VCDs and mixing ratios over Pune during the monsoon season were filtered based on MAPA-generated profile parameters. Cloud cover and high AOD filters were responsible for most such filtering. Only one valid CHOCHO VCD and mixing ratio profile was available from Pune during the monsoon season on June 5, 2018, which is at the beginning of the monsoon season. Hence, seasonal and diurnal variations of CHOCHO VCDs and mixing ratios over Pune will not be discussed for monsoon season; rather, the result from the one observation will be mentioned with relevant context. The average CHOCHO VCD over Pune (all seasons) was $1.52 \pm 0.66 \times 10^{15}$ molec. cm^{-2} with a range between 0.06 and 5.34×10^{15} molec. cm^{-2}. Delhi showed the highest average CHOCHO VCD among the three locations with $1.57 \pm 0.98 \times 10^{15}$molec. cm^{-2} (range: 0.06–4.87 $\times 10^{15}$ molec. cm^{-2}). Mahabaleshwar showed the lowest average CHOCHO VCD of $0.66 \pm 0.40 \times 10^{15}$ molec. cm^{-2} with a range of 0.13–1.95 $\times 10^{15}$ molec. cm^{-2}.

CHOCHO vmr in Pune ranges from 0.02 to 2.12 ppb with an average (all seasons) of 0.33 ± 0.18 ppb. In Delhi the typical vmr ranged between 0.10 and 1.62 ppb with a higher typical average value (compared to Pune) of 0.43 ± 0.27 ppb. However, for one day (June 09, 2019) high CHOCHO vmr of up to 1.63 ppb was observed in Delhi. Among the three sites, Mahabaleshwar showed the lowest average CHOCHO vmr of 0.08 ± 0.03 ppb (range: 0.01–0.18 ppb).

4. Discussions

4.1. Seasonal and diurnal variation of CHOCHO

Fig. 4a and b shows the seasonal and monthly average CHOCHO VCDs from the three sites. Observations from Pune spanned over three seasons (only one valid observation during the monsoon season). In contrast, observations from Mahabaleshwar and Delhi spanned over one season (pre-monsoon and monsoon seasons, respectively). The highest average seasonal VCD ($1.75 \pm 0.63 \times 10^{15}$ molec. cm^{-2}) over Pune was found during winter. The highest monthly average VCD ($1.82 \pm 0.62 \times 10^{15}$ molec. cm^{-2}) was observed in January, and the lowest ($0.79 \pm 0.45 \times 10^{15}$ molec. cm^{-2}) during May. The seasonal variation shows higher VCD during winter and post-monsoon seasons. However, only one valid MAPA result is available over Pune during monsoon season. Hence the higher VCD observation during winter and post-monsoon could be due to sampling bias. Occasional high CHOCHO VCDs were observed during the pre-monsoon period; however, the mean VCD level remained lower than in the winter and post-monsoon seasons. Similar observations of higher CHOCHO VCDs during winter were reported by Javed et al. (2019a) over Beijing and Baoding, China and by Benavent et al. (2019) over Madrid, Spain. Javed et al. (2019a) suggested the

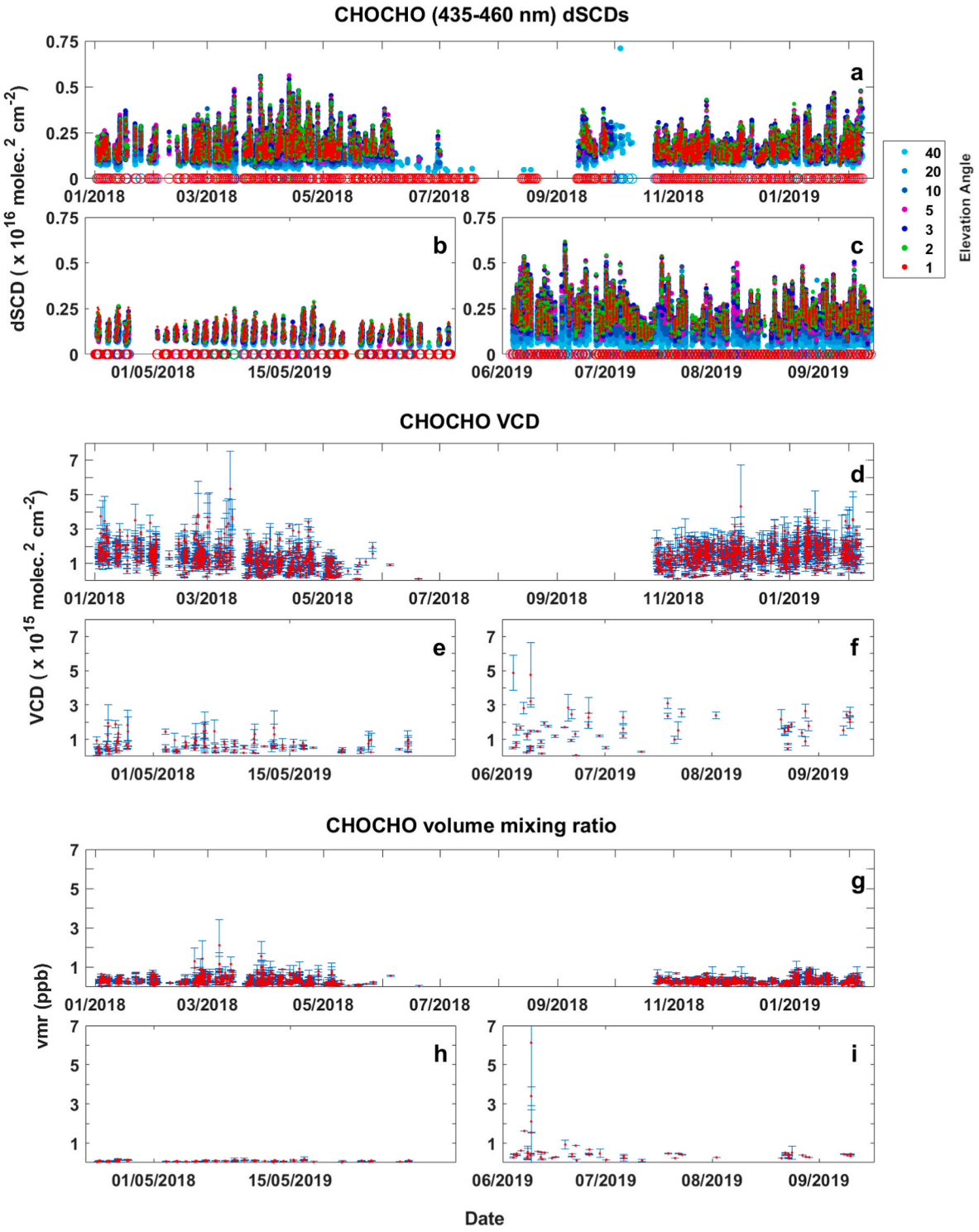

Fig. 3. dSCD, VCD and vmr time-series of CHOCHO from the three observation sites (Pune city, Mahabaleshwar and Delhi). Panels 'a', 'b' and 'c' show the dSCD time-series from Pune city, Mahabaleshwar and Delhi, respectively. Different colored solid (hollow) circles represent CHOCHO dSCDs above (below) detection limit at different elevation angles. Panels 'd', 'e' and 'f' show CHOCHO VCD time-series (retrieved from MAPA using dSCDs) from Pune city, Mahabaleshwar and Delhi, respectively, along with the VCD errors. Panel 'g', 'h', and 'i' shows surface CHOCHO vmr timeseries from Pune city, Mahabaleshwar and Delhi, respectively, along with the associated errors.

presence of anthropogenic precursors (Liu et al., 2012; Myriokefalitakis et al., 2008), like acetylene and benzene, and their oxidation to CHOCHO is responsible for higher winter VCDs.

Over Delhi, the average VCD during monsoon was higher than any other season in other locations. Delhi, the capital of India with a higher population than Pune, experience higher anthropogenic emission. During monsoons, under cloudy sky conditions, CHOCHO sink via photolysis reduces due to less availability of solar radiation increasing CHOCHO lifetime. Both these factors lead to a higher average CHOCHO VCD over Delhi during monsoon. Javed et al. (2019b) reported higher CHOCHO on hazy and cloudy days in Beijing, China, compared to clear sky days due to slower photolysis.

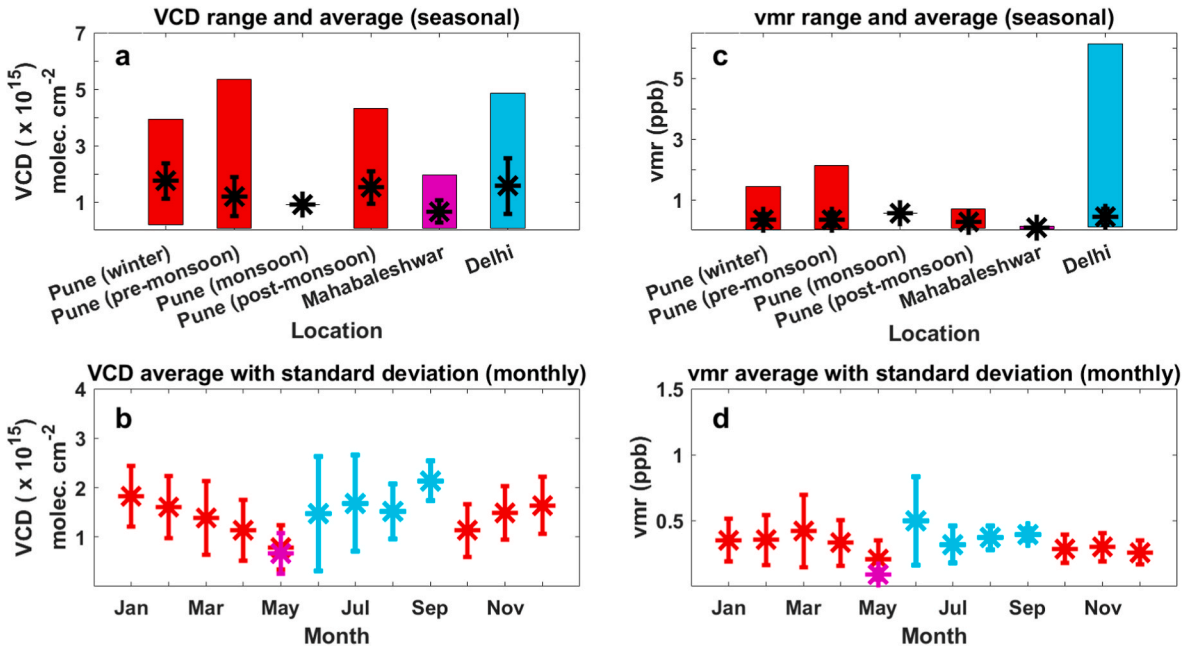

Fig. 4. Seasonal and monthly average of CHOCHO VCD (panels 'a' and 'b') and surface vmr (panels 'c' and 'd') from Pune city (red), Mahabaleshwar (magenta) and Delhi (cyan) respectively. Panels 'a' and 'c' show the seasonal mean with standard deviation (asterisk and error bars) and the range of CHOCHO (bars) for CHOCHO VCD and surface vmr, respectively. Panels 'b' and 'd' show the monthly mean with standard deviation (asterisk and error bar) for CHOCHO VCD and surface vmr, respectively.

Mahabaleshwar showed a lower monthly average VCD than Pune during May. It also showed a lower pre-monsoon average VCD than Pune. The lowest average CHOCHO VCD (and smallest range) in Mahabaleshwar compared to the other locations indicates lower CHOCHO precursors in the atmosphere. As Mahabaleshwar is a forested region with lower CHOCHO VCD, the anthropogenic sources of CHOCHO precursor in Pune and Delhi are much stronger than biogenic sources at Mahabaleshwar. Additionally, being a high-altitude location, the observation site at Mahabaleshwar remains above the boundary layer in the early morning (Biswas et al., 2021). The MAX-DOAS observations in the early morning samples the free troposphere with lower CHOCHO. The boundary layer height increases till 3 p.m. due to solar heating. Hence, as the day progresses, the MAX-DOAS observations sample air within the boundary layer, eventually showing increasing CHOCHO levels. Similar observations were reported for nitrogen dioxide (NO_2) and formaldehyde (HCHO) over Mahabaleshwar (Biswas et al., 2021).

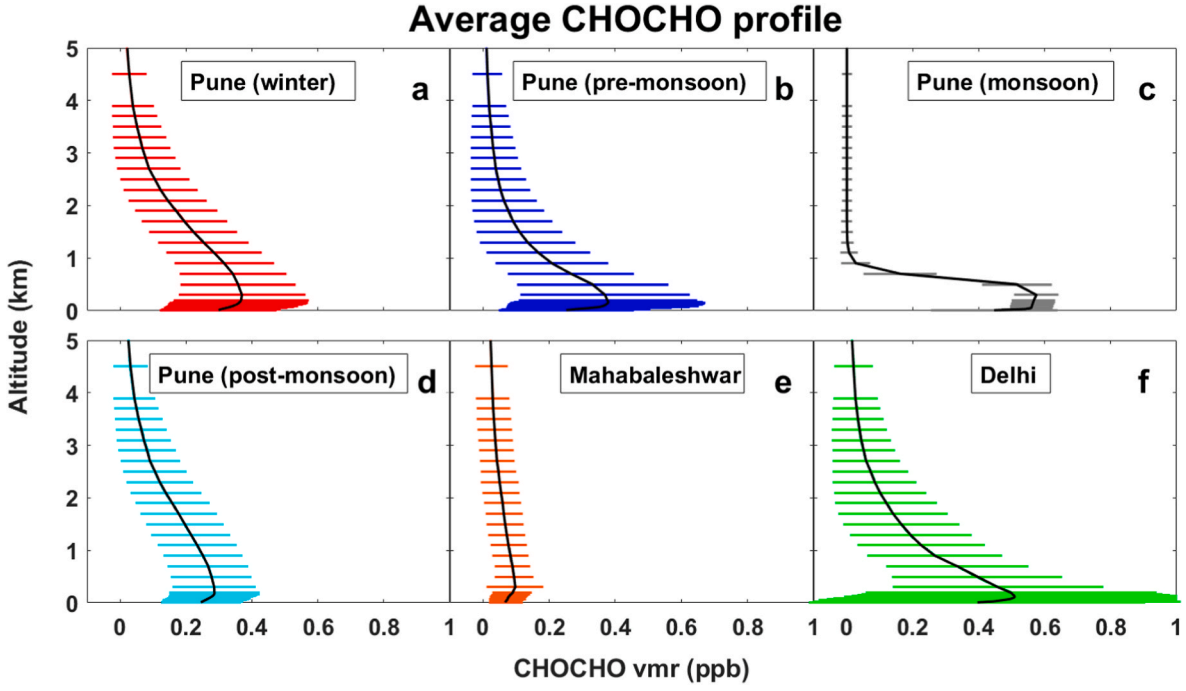

Fig. 5. Average CHOCHO vertical profiles from Pune city, Mahabaleshwar, and Delhi, respectively. Panel 'a', 'b', 'c' and 'd' show the average seasonal vertical profiles and standard deviations (except monsoon, as only one valid profile was available, and hence the error is shown) over Pune. Panels 'e' and 'f' show average seasonal vertical profiles with standard deviations over Mahabaleshwar and Delhi, respectively.

Fig. 4c and d shows the seasonal and monthly average CHOCHO surface vmr over the observation sites. The average seasonal vmr during winter (0.35 ± 0.17 ppb) and pre-monsoon (0.35 ± 0.23 ppb) seasons are similar over Pune. The highest average vmr was observed during monsoon, but as only one valid vmr is available, we should not consider this a seasonal average. Post-monsoon (0.28 ± 0.10 ppb) average vmr was the lowest over Pune among all the seasons. March shows the highest monthly vmr (0.43 ± 0.28 ppb), whereas May shows the lowest (0.20 ± 0.15 ppb). The typical average CHOCHO vmr (0.43 ± 0.27 ppb) was high in Delhi. The range of values in Delhi was higher than Pune. Due to a lack of valid observations over Pune during monsoon, a direct comparison is not possible. Mahabaleshwar showed the lowest average CHOCHO vmr (0.08 ± 0.03 ppb) among the three locations.

Fig. 5 shows the seasonal average CHOCHO vertical profiles from all observation sites. Fig. 5a–d shows the average profile (with standard deviations) from winter, pre-monsoon, monsoon and post-monsoon over Pune. CHOCHO mixing ratio increases with altitude up to ~190–300 m from the surface and then decreases. During pre-monsoon season the highest mixing ratio at ~190 m (0.38 ± 0.27 ppb) is observed. This explains the highest surface mixing ratio during March, which is averaged only up to ~200 m altitude. Above ~200 m from the surface CHOCHO mixing ratio decreases rapidly during pre-monsoon season, whereas the decrease is more gradual during winter and post-monsoon. The average profile height was lower during the pre-monsoon season than in the winter and post-monsoon. During pre-monsoon season photolysis rate of CHOCHO is higher due to the availability of solar radiation compared to winter and post-monsoon. This is probably the reason for the rapid decrease in the CHOCHO mixing ratio with altitude in pre-monsoon. The lowest profile height was observed during monsoon season, but we have only one valid profile during monsoon. Unlike the monsoon profile from Pune, the average profile from Delhi does not show a lower profile height during monsoon. Delhi also shows higher CHOCHO vmr at lower altitudes (Fig. 5f).

Fig. 6 shows the diurnal variation of CHOCHO VCD and vmr from Pune city, Mahabaleshwar and Delhi. As only one valid VCD was available during the monsoon period, an average diurnal profile could not be prepared. During all the seasons in Pune, CHOCHO increases gradually in the morning, reaching peak value around noon (~11 a.m.–12 p.m.) and then gradually decreasing later in the day (reaching a lower value during ~4–5 p.m.). This indicates a typical photochemistry-driven CHOCHO diurnal profile. During the daytime, biogenic and anthropogenic VOCs get photo-oxidized, leading to peak value around noon. In the morning, emissions from automobiles peak at ~9–10 a.m. Hence, considering the lifetime of the precursor species, higher CHOCHO VCD around noon is expected. During the afternoon, the photochemical loss of CHOCHO exceeds production, resulting in decreasing VCD. Over Delhi, CHOCHO VCD increases in the morning, reaching maxima at ~11 a.m. However, no average hourly data is available during 12–4 pm. At ~5 p.m., a lower CHOCHO VCD value indicates possible VCD diurnal variation similar to Pune. These patterns again show photochemistry-driven diurnal variation. The correlation between hourly averaged CHOCHO VCDs and hourly averaged surface downward short-wave radiation flux over Pune showed a positive correlation (Fig. 7a; $r = 0.62$, $p < 0.01$). This agrees with the role of active photochemistry determining the diurnal variation of CHOCHO. Fig. 7b shows diurnal variation of these two parameters over one example day (November 13, 2018). The figure also shows that the diurnal trend of CHOCHO closely matches the solar radiation, showing that photochemistry is an important factor in determining the variation.

Fig. 6f–j shows the average surface CHOCHO vmr diurnal profile from all seasons. Unlike the symmetrical diurnal profile of CHOCHO VCDs, CHOCHO vmr increases faster in the morning and reaches the day high ~11 a.m. Then the vmr decreases slowly, and during the afternoon, it reaches an even lower value compared to the morning. CHOCHO VCDs are representative of the total CHOCHO present in the atmosphere over the observation site. However, surface mixing ratios are representative of concentrations in the lowest layer. As explained earlier, the boundary layer height starts to increase due to heating by solar radiation leading to an increase in its thickness. Due to this, the surface vmr decreases even though the VCDs show an increase. Additionally, as emissions reduce later in the day due to lower traffic-based emissions, the photochemical removal process of CHOCHO starts to dominate, leading to a decrease in surface vmr. NO_2 is an indicator of emissions from the transport sector, power and heavy industrial sectors, and over Pune, NO_2 displays distinct peaks in the morning and evening during peak traffic hours (Biswas and Mahajan, 2021). CHOCHO and NO_2 VCDs from Pune also showed a positive correlation ($r = 0.49$, $p < 0.01$). This suggests an effect of transport emissions on CHOCHO. However, NO_2 and CHOCHO have different chemistry and lifetimes in the atmosphere, affecting their formation and sinks. Hence, a perfect match between CHOCHO and NO_2

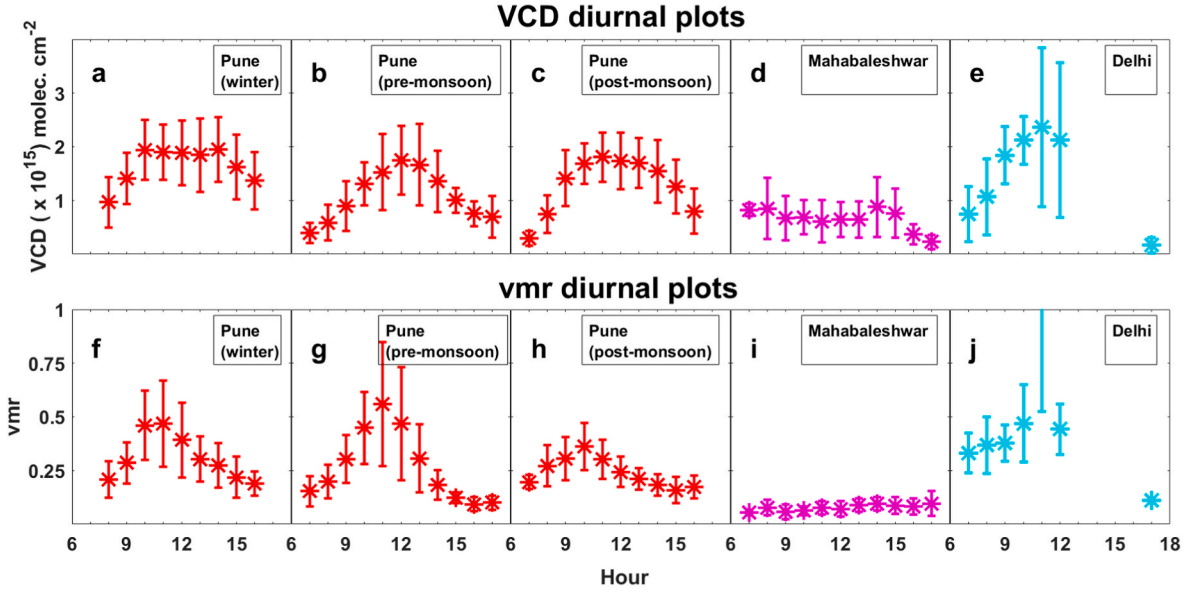

Fig. 6. CHOCHO VCD and vmr diurnal plots from Pune city, Mahabaleshwar, and Delhi. Panel 'a' ('f'), 'b' ('g'), 'c' ('h'), 'd' ('i') and 'e' ('j') show seasonal average VCD (vmr) diurnal plots from Pune-winter, Pune-pre-monsoon, Pune-post-monsoon, Mahabaleshwar and Delhi. No seasonal, diurnal plot from Pune-monsoon was shown, as only one valid VCD (vmr) was available.

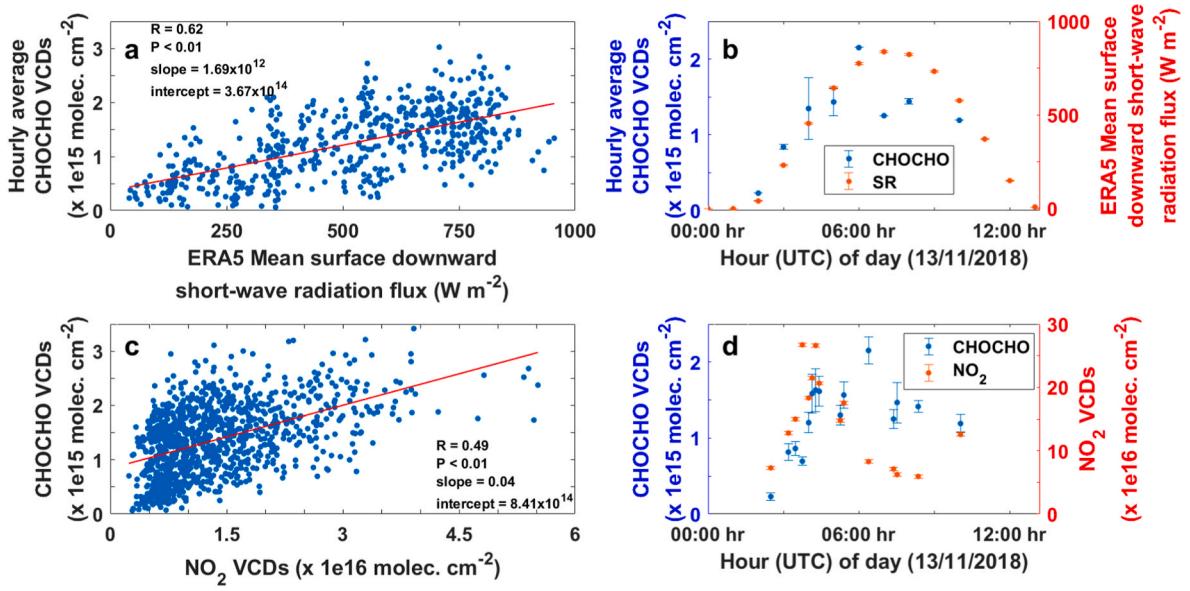

Fig. 7. Correlation between the hourly averaged CHOCHO VCDs and the hourly averaged surface downward short-wave radiation (ERA5 reanalysis) is shown in panel **'a'.** There is a positive correlation between these two variables, indicating a photochemistry driven CHOCHO diurnal profile. Panel '**b**' shows the diurnal variation of hourly average CHOCHO and hourly averaged surface downward short-wave radiation on an example day, November 13, 2018. Panel '**c**' shows the correlation between CHOCHO and NO_2 VCDs. Positive correlation between CHOCHO and NO_2 and VCDs suggests similar sources related to traffic emission for both the trace gases. Panel '**d**' shows CHOCHO and NO_2 VCDs from November 13, 2018.

is not expected. Fig. 7c presents a scatter plot of NO_2 and CHOCHO VCDs, which shows a moderate correlation with a large spread. Fig. 7d presents CHOCHO and NO_2 VCDs from November 13, 2018. CHOCHO and NO_2 follow a similar trend in the morning, but after peak traffic hours, NO_2 values fall sharply as NO_2 photochemically decomposes faster than its production. However, due to the slower conversion of VOCs to CHOCHO, the CHOCHO VCDs continue to increase, peaking later in the day. By contrast, an increasing CHOCHO surface vmr was observed in Mahabaleshwar throughout the day (Fig. 6i), similar to as reported by Biswas et al. (2021) for nitrogen dioxide and formaldehyde diurnal profile over Mahabaleshwar (explained above). However, considering the standard deviation associated with the hourly average mixing ratio, the increase is not significant. An increasing trend of CHOCHO surface vmr in the morning was observed over Delhi (Fig. 6j) with a high value during 11 a.m., indicating a traffic emission-related CHOCHO profile.

We studied the effect of open biomass burning around Pune City on CHOCHO mixing ratios. Biswas and Mahajan (2021) studied the effect of open biomass burning on HCHO and NO_2 mixing ratio over Pune City. The pre-monsoon season over Pune experiences a peak in open biomass burning. Hence, Biswas and Mahajan (2021) have studied the effect of open biomass burning only during pre-monsoon season. Using HYSPLIT back trajectories and satellite observations for fire events, they identified air parcels that had flown over a fire event in the last 12 h. Depending on the exposure to fires, the corresponding air parcels were checked for increase in NO_2 and HCHO. They reported that air parcels exposed to fires corresponded to higher NO_2 and HCHO mixing ratios. Following a similar argument, we have done a analysis to identify if fires had an impact on the CHOCHO observations. We have identified the air parcels reaching Pune City, which had flown over fire events in the past 12 h during the pre-monsoon season. The CHOCHO observations with the corresponding air parcels were checked for anomalous CHOCHO levels. However, no conclusive results were obtained from this study. The diurnal profile of CHOCHO mixing ratios corresponding to 'all fire' and 'no fire' events do not show conclusive differences. Fig. S1 shows the results of the study. The lack of enough CHOCHO observation is probably responsible for the inconclusive result.

On June 9, 2019, elevated CHOCHO vmr (up to 6.13 ppb (at ~11:00–11:30 a.m.) compared to typical average of 0.43 ± 0.27 ppb), was observed over Delhi (Fig. 8). We compared ambient $PM_{2.5}$ and PM_{10} data from a nearby air quality monitoring site and found a spike during the same period. However, other observation sites around Delhi did not show a similar spike in $PM_{2.5}$ and PM_{10}. Concurrent high values in CHOCHO surface vmr and surface particulate matter concentration indicate a local emission event, like open biomass burning. CHOCHO vertical profiles from that period also show high CHOCHO in the lower atmospheric levels.

To identify the interaction between aerosols and CHOCHO, we studied the correlation between CHOCHO and AOD. Previous studies have suggested glyoxal as a potential precursor for secondary organic aerosol formation (Rossignol et al., 2014; Volkamer et al., 2007; Washenfelder et al., 2011). Schweitzer et al. (1998) reported that CHOCHO gets scavenged by cloud droplets and fog. However, Javed et al. (2019b) reported that CHOCHO concentrations are higher on haze days due to lower atmospheric oxidation and photolysis rates. A positive correlation between CHOCHO VCDs and AERONET AOD at 440 nm was observed over Pune ($r = 0.35$, $p < 0.01$; Fig. S2a). However, although there was a positive correlation across the campaign, there was considerable differences during different periods. During January 2018, both CHOCHO VCD and AOD showed high values. During February and March 2018, CHOCHO VCDs and AOD showed an opposite trends, where CHOCHO VCDs decreased gradually through February and March 2018 but AOD was higher in March 2018 than in February 2018. In January 2019, CHOCHO VCDs showed similar levels to January 2018 but AOD in January 2019 was lower than in January 2018 (Fig. S2b). Hence, the high CHOCHO during winter is not solely due to high AOD or indeed the cause of higher aerosol loading. This analysis indicates a possible relationship between the CHOCHO and heterogeneous chemistry across the campaign, but the true nature is not clear. Long-term studies with detailed observations of aerosol types needs to be performed to understand the relationship between CHOCHO and aerosol.

4.2. Comparison with satellite data

CHOCHO VCDs over Pune, Mahabaleshwar and Delhi (averaged over a 20 km radius around the observation site) were compared with S5P

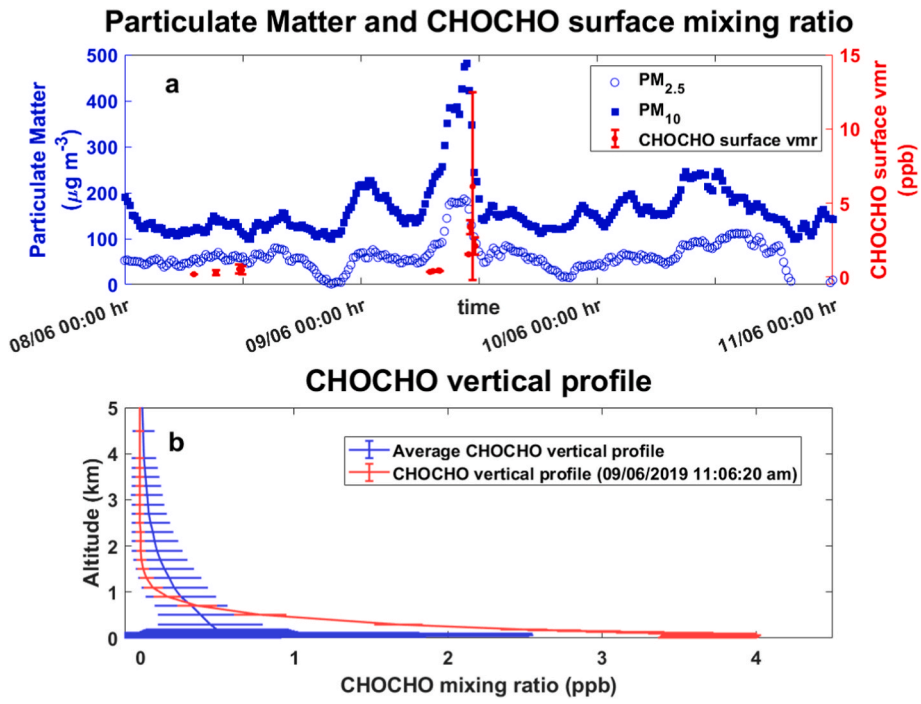

Fig. 8. Panel 'a' shows timeseries of $PM_{2.5}$ (hollow circle), PM_{10} (solid square) and CHOCHO surface mixing ratio (red dot) for 08–10/06/2019 over Delhi. High $PM_{2.5}$, PM_{10} and CHOCHO surface mixing ratio were observed on June 09, 2019. Panel 'b' shows vertical profile of CHOCHO mixing ratios for total campaign average (blue) and on June 09, 2019 11:06:20 a.m. (red) corresponding to a high CHOCHO surface vmr observation. Profile with high surface CHOCHO mixing ratio shows high CHOCHO levels in the lower atmospheric layers but drops sharply with altitude.

satellite CHOCHO VCDs. Fig. 9a shows the monthly average CHOCHO VCDs observed by the S5P satellite and from the MAPA analysis. The monthly average VCDs over Pune (red line) show prominent monthly variation with high values during winter and post-monsoon months and a minimum during monsoon. This observation is similar to the ground-based observations over Pune. The highest monthly average CHOCHO VCD from S5P observation was found during January. However, the average S5P VCD value ($0.73 \pm 0.30 \times 10^{15}$ molec. cm^{-2}) during January is lower than the ground-based observation ($1.8 \pm 0.62 \times 10^{15}$ molec. cm^{-2}). For all the months, the satellite observations underestimated CHOCHO compared to ground-based observations over Pune. Underestimation of CHOCHO VCD by S5P satellite was found over Delhi also. The average seasonal VCD (ground-based) over Delhi was 1.6×10^{15} molec. cm^{-2} whereas the highest monthly average S5P CHOCHO VCD (during June) was 0.64×10^{15} molec. cm^{-2}. Over Mahabaleshwar also, underestimation by S5P compared to ground-based CHOCHO VCDs were found (S5P average VCD: $0.43 \pm 0.20 \times 10^{15}$ molec. cm^{-2}; ground-based average VCD: $0.66 \pm 0.40 \times 10^{15}$ molec. cm^{-2}).

We studied the correlation between satellite VCDs and ground-based VCDs over Pune, as only this site has enough collocated data from both satellite and ground-based observations. We used the spatial average of S5P CHOCHO VCD from a 20 km radius around the observation site for the correlation. The temporal average of ground-based CHOCHO VCD within ±30 min windows of daily local satellite overpass time was used. Fig. 9b shows the results of the correlation study. A total of 32 data points were used for this study. A poor positive correlation was found ($r = 0.262$, $p = 0.148$). Fig. 10b and c shows that S5P systematically underestimates CHOCHO VCD compared to ground-based observations. From the seven collocated data points from Mahabaleshwar (not shown in the plot), an underestimation of S5P is also evident. Ground-based MAX-DOAS observations are more sensitive towards lower atmospheric layers. As CHOCHO sources are predominantly situated near the surface, the ground-based MAX-DOAS observations capture the concentrations better than the satellite. In a recent study, Lerot et al. (2021) reported the first global CHOCHO column products from TROPOMI satellite. TROPOMI CHOCHO columns were validated using ground-based MAX-DOAS observations from two different Indian stations in Northern India, Mohali and Pantnagar. Both stations experience seasonal variability due to biomass burning and monsoon, which were captured well in satellite and ground-based observations. However, TROPOMI observations underestimated CHOCHO VCDs compared to MAX-DOAS observations. The probable reasons for the underestimation were sampling of different airmass, different instrument vertical sensitivity, and different DOAS data analysis approaches. We have also compared the satellite a priori CHOCHO profile (Lerot et al., 2021) with MAPA retrieved profiles. CHOCHO a priori profiles show similar vertical distribution compared to the MAPA retrieved profiles. However, the CHOCHO concentration at different vertical levels was higher (~5 times at the surface level) for MAPA retrieved profiles compared to the a priori. Lower CHOCHO in the a priori can be another reason for the satellite underestimation.

4.3. Comparison with previous studies

In this section, we compare the CHOCHO results from the present study with previous studies. Table 3 and Fig. 10 compare previous DOAS-based CHOCHO studies from ground-based and air-borne observations around the world. In this section, the serial numbers from Table 3 and Fig. 10 corresponding to previous studies are mentioned within the parentheses while discussing. Readers are requested to follow Table 3 and Fig. 10 with the corresponding serial numbers. DOAS observations from urban environments have shown higher CHOCHO levels than remote environments. CHOCHO observations from urban Pune city (no. 18) and Delhi city (sr. no. 20) are comparable to previous CHOCHO studies in urban environments as mentioned in Table 3 and Fig. 10. However, Delhi shows the highest average surface mixing ratios among all the previous reports. Observations from Mainz, Germany (up to 1.40×10^{16} molec. cm^{-2}, sr. no. 3 b) and Islamabad, Pakistan (up to 7.81×10^{15}molec. cm^{-2}, sr. no. 3 b) show higher VCDs compared to Pune and Delhi. Average CHOCHO VCD of Pune ($1.52 \pm 0.66 \times 10^{15}$ molec.

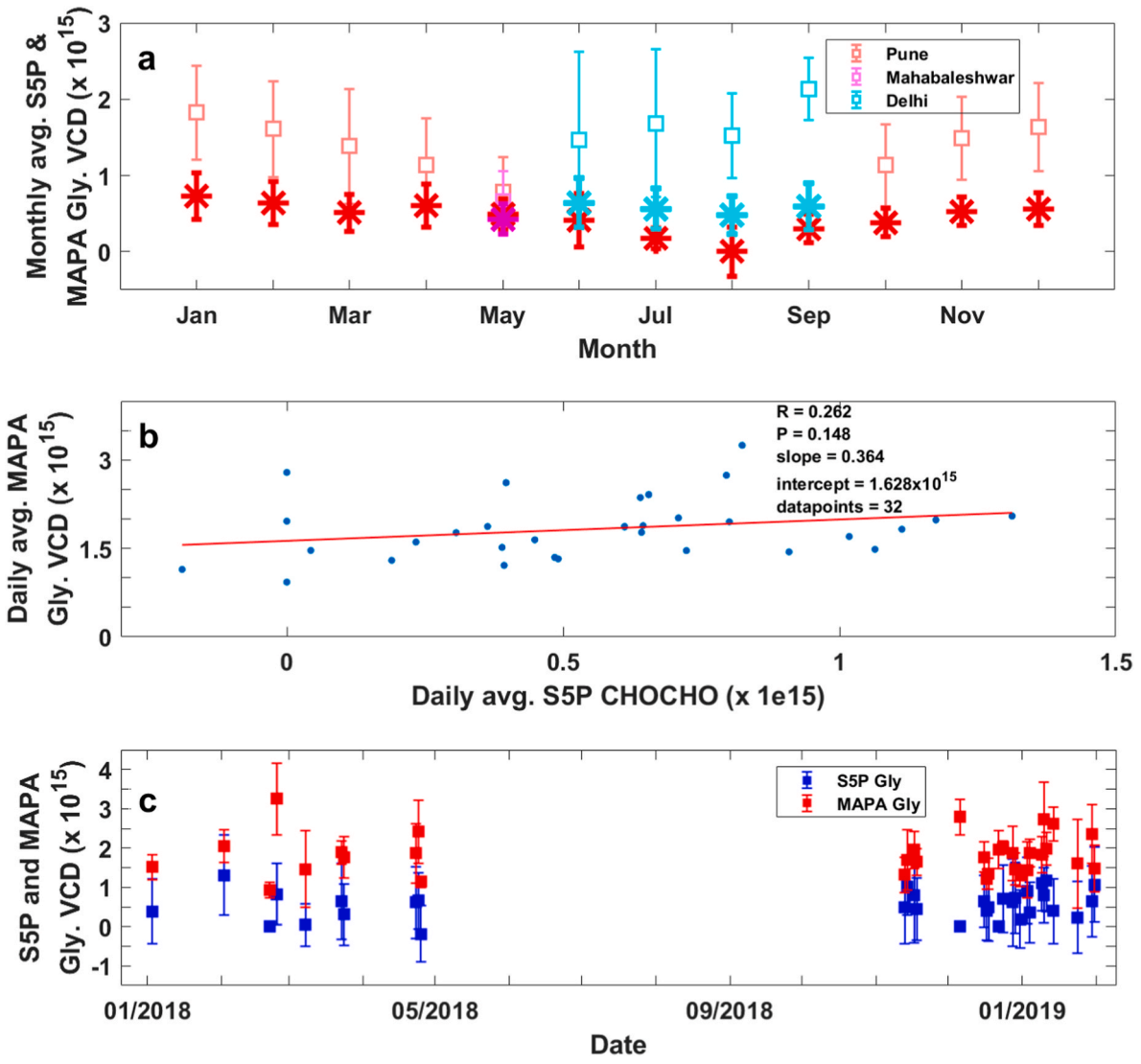

Fig. 9. Panel 'a' shows monthly average CHOCHO VCDs with standard deviations from S5P satellite (asterisk) and MAX-DOAS (square) over Pune city (red), Mahabaleshwar (magenta), and Delhi (cyan). Panel 'b' shows a scatter plot of collocated average CHOCHO VCDs from ground-based (averaged over ± 30 min windows of daily local satellite overpass time) and satellite observations (daily averaged over a 20 km radius around the observation site) over Pune. Panel 'c' shows time-series plot of collocated CHOCHO VCDs from ground-based (red) and satellite (blue) observations over Pune.

cm^{-2}), Delhi ($1.60 \pm 0.98 \times 10^{15}$ molec. cm^{-2}) and Athens ($1.80 \pm 0.80 \times 10^{15}$molec. cm^{-2}) were found to be comparable. Beijing (China), Baoding (China), Madrid (Spain), Vienna (Austria), and Pune (India) showed higher CHOCHO during winter and lower CHOCHO during summer, indicating predominant anthropogenic precursors for CHOCHO. CHOCHO from Athens showed higher values during summer, indicating predominant biogenic sources.

Observations from remote environments have shown lower CHOCHO levels than urban environments (Table 3). Forested regions (California, USA (0.27 ± 0.03 ppb), Borneo rainforest (up to 1.6 ppb), and Amazon basin (0.09–0.25 ppb)) have shown the highest CHOCHO levels among different remote environments. Except for the Borneo rainforest, CHOCHO values at Mahabaleshwar were similar to other forested regions worldwide. Mahabaleshwar observations are comparable to CHOCHO observations from rural Phimai (Thailand) and Changshou (China).

5. Conclusions

We present MAX-DOAS observations of atmospheric CHOCHO from three different locations in Pune: Pune city, Mahabaleshwar and Delhi. Mahabaleshwar represents a rural forested environment, whereas Pune city and Delhi represent urban environments. Delhi and Mahabaleshwar showed the highest and lowest average CHOCHO VCD and vmr among the three observation sites. Similar results were found from S5P satellite-measured CHOCHO VCDs, indicating anthropogenic emissions significantly contribute to CHOCHO concentration over the observation sites. Ground-based and satellite observations have confirmed that the monthly average CHOCHO VCD over Pune is highest during January and then decreases to a minimum in August (for ground-based observations minimum is observed in May as only one single VCD was available during June–September), and then again increase till December. Earlier studies have suggested that this pattern indicates an anthropogenic emission-dominated CHOCHO profile. No significant monthly variation in CHOCHO vmr was observed. In Pune and Delhi, CHOCHO VCDs and surface mixing ratios show lower values in the early morning and increase until noon. CHOCHO VCDs and surface mixing ratios decrease later in the day, leading to a lower value in the afternoon. This shows a photochemistry-driven CHOCHO diurnal profile. CHOCHO over Mahabaleshwar shows an increasing profile throughout the day, indicating the effect of boundary layer evolution. The S5P observations have been found to systematically underestimate atmospheric CHOCHO

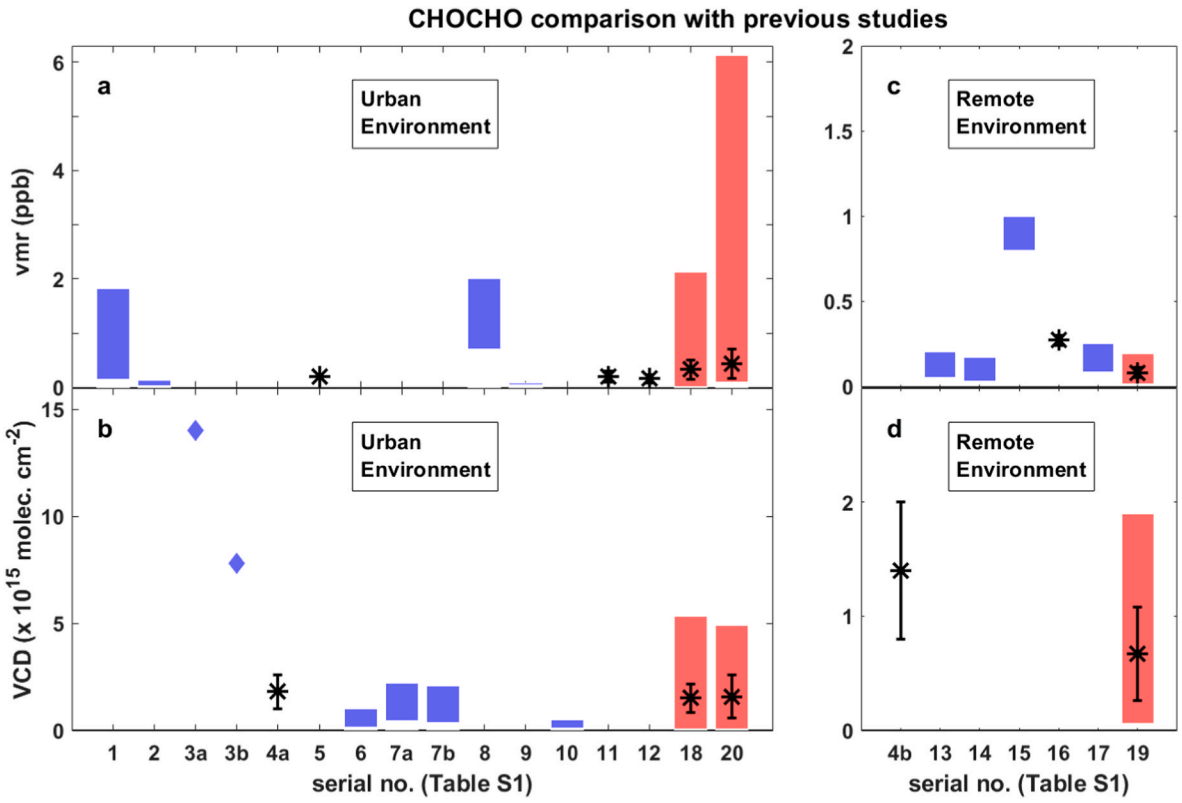

Fig. 10. Comparative plot of CHOCHO VCD and vmr from previous studies with respect to the present study. The serial numbers represent different observation sites from different campaigns. Details of those sites are available in Table 3. Blue (Red) bars represent the range of CHOCHO VCD/vmr from previous (present) studies. Panel 'a' ('b') and 'c' ('d') represents CHOCHO mixing ratio (VCD) from urban and remote environment respectively. The asterisks with lines show the average VCD/vmr values and the standard deviation. The blue diamond symbols represent the CHOCHO observations only with upper limits.

VCDs compared to ground-based observations. Ground-based MAX-DOAS observations are more sensitive towards lower atmospheric layers. As most CHOCHO concentrations are found near the surface (as evident from CHOCHO vertical profile) due to the higher availability of precursors from emission, ground-based observations capture surface CHOCHO concentration better than satellites. CHOCHO VCDs and surface mixing ratio over Pune and Delhi showed comparable results from other urban environments worldwide. CHOCHO levels from Mahabaleshwar showed comparable results from other forested regions worldwide.

CRediT authorship contribution statement

Mriganka Sekhar Biswas: Formal analysis, Writing – original draft. **Prithviraj Mali:** Formal analysis. **Christophe Lerot:** Satellite data analysis. **Isabelle De Smedt:** Satellite data analysis. **Anoop S. Mahajan:** Conceptualization, Instrumentation, Software, Formal analysis, Writing – review & editing.

Declaration of competing interest

The authors declare the following financial interests/personal relationships which may be considered as potential competing interests: Anoop Sharad Mahajan reports financial support was provided by Indian Institute of Tropical Meteorology. Anoop Mahajan reports a relationship with Indian Institute of Tropical Meteorology that includes: employment.

Data availability

Data will be made available on request.

Acknowledgements

IITM is funded by the Ministry of Earth Sciences, Government of India.

Appendix A. Supplementary data

Supplementary data to this article can be found online at https://doi.org/10.1016/j.atmosenv.2023.120109.

References

Alvarado, L.M.A., Richter, A., Vrekoussis, M., Hilboll, A., Kalisz Hedegaard, A.B., Schneising, O., Burrows, J.P., 2020. Unexpected long-range transport of glyoxal and formaldehyde observed from the Copernicus Sentinel-5 Precursor satellite during the 2018 Canadian wildfires. Atmos. Chem. Phys. 20, 2057–2072. https://doi.org/10.5194/acp-20-2057-2020.

Alvarado, L.M.A., Richter, A., Vrekoussis, M., Wittrock, F., Hilboll, A., Schreier, S.F., Burrows, J.P., 2014. An improved glyoxal retrieval from OMI measurements. Atmos. Meas. Tech. 7, 4133–4150. https://doi.org/10.5194/amt-7-4133-2014.

Baidar, S., Oetjen, H., Coburn, S., Dix, B., Ortega, I., Sinreich, R., Volkamer, R., 2013. The CU Airborne MAX-DOAS instrument: vertical profiling of aerosol extinction and trace gases. Atmos. Meas. Tech. 6, 719–739. https://doi.org/10.5194/amt-6-719-2013.

Beirle, S., Dörner, S., Donner, S., Remmers, J., Wang, Y., Wagner, T., 2019. The Mainz profile algorithm (MAPA). Atmos. Meas. Tech. 12, 1785–1806. https://doi.org/10.5194/amt-12-1785-2019.

Benavent, N., Garcia-Nieto, D., Wang, S., Saiz-Lopez, A., 2019. MAX-DOAS measurements and vertical profiles of glyoxal and formaldehyde in Madrid, Spain. Atmos. Environ. 199, 357–367. https://doi.org/10.1016/j.atmosenv.2018.11.047.

Biswas, M.S., Ghude, S., Gurnale, D., Prabhakaran, T., Mahajan, A.S., 2019. Simultaneous observations of nitrogen dioxide, formaldehyde and ozone in the Indo-Gangetic Plain. Aerosol Air Qual. Res. 19, 1749–1764. https://doi.org/10.4209/aaqr.2018.12.0484.

Biswas, M.S., Mahajan, A.S., 2021. Year-long concurrent MAX-DOAS observations of nitrogen dioxide and formaldehyde at Pune: understanding diurnal and seasonal variation drivers. Aerosol Air Qual. Res. 21 https://doi.org/10.4209/aaqr.200524.

Biswas, M.S., Pandithurai, G., Aslam, M.Y., Patil, R.D., Anilkumar, V., Dudhambe, S.D., Lerot, C., De Smedt, I., Van Roozendael, M., Mahajan, A.S., 2021. Effect of boundary layer evolution on nitrogen dioxide (No2) and formaldehyde (hcho) concentrations at a high-altitude observatory in western India. Aerosol Air Qual. Res. 21, 1–21. https://doi.org/10.4209/aaqr.2020.05.0193.

Chance, K., Kurucz, R.L., 2010. An improved high-resolution solar reference spectrum for earth's atmosphere measurements in the ultraviolet, visible, and near infrared. J. Quant. Spectrosc. Radiat. Transf. 111, 1289–1295. https://doi.org/10.1016/j.jqsrt.2010.01.036.

Chowdhury, S., Dey, S., Tripathi, S.N., Beig, G., Mishra, A.K., Sharma, S., 2017. "Traffic intervention" policy fails to mitigate air pollution in megacity Delhi. Environ. Sci. Pol. 74, 8–13. https://doi.org/10.1016/j.envsci.2017.04.018.

Clémer, K., Van Roozendael, M., Fayt, C., Hendrick, F., Hermans, C., Pinardi, G., Spurr, R., Wang, P., De Mazière, M., 2010. Multiple wavelength retrieval of tropospheric aerosol optical properties from MAXDOAS measurements in Beijing. Atmos. Meas. Tech. 3, 863–878. https://doi.org/10.5194/amt-3-863-2010.

Danckaert, T., Fayt, C., Van Roozendael, M., De Smedt, I., Letocart, V., Merlaud, A., Pinardi, G., 2014. QDOAS Software User Manual.

Deutschmann, T., Beirle, S., Frieß, U., Grzegorski, M., Kern, C., Kritten, L., Platt, U., Prados-Román, C., Pukite, J., Wagner, T., Werner, B., Pfeilsticker, K., 2011. The Monte Carlo atmospheric radiative transfer model McArtim: introduction and validation of Jacobians and 3D features. J. Quant. Spectrosc. Radiat. Transf. 112, 1119–1137. https://doi.org/10.1016/j.jqsrt.2010.12.009.

Draxler, R.R., Hess, G.D., 1998. An overview of the HYSPLIT_4 modelling System for trajectories, dispersion, and deposition. Aust. Meteorol. Mag. 47, 295–308.

Fayt, C., Van Roozendael, M., 2013. QDOAS 1.00. Software User Manual [WWW Document].

Fleischmann, O.C., Hartmann, M., Burrows, J.P., Orphal, J., 2004. New ultraviolet absorption cross-sections of BrO at atmospheric temperatures measured by time-windowing Fourier transform spectroscopy. J. Photochem. Photobiol. Chem. 168, 117–132. https://doi.org/10.1016/j.jphotochem.2004.03.026.

Fu, D., Millet, D.B., Wells, K.C., Payne, V.H., Yu, S., Guenther, A., Eldering, A., 2019. Direct retrieval of isoprene from satellite-based infrared measurements. Nat. Commun. 10 https://doi.org/10.1038/s41467-019-11835-0.

Fu, T.M., Jacob, D.J., Wittrock, F., Burrows, J.P., Vrekoussis, M., Henze, D.K., 2008. Global budgets of atmospheric glyoxal and methylglyoxal, and implications for formation of secondary organic aerosols. J. Geophys. Res. Atmos. 113.

Gratsea, M., Vrekoussis, M., Richter, A., Wittrock, F., Schönhardt, A., Burrows, J., Kazadzis, S., Mihalopoulos, N., Gerasopoulos, E., 2016. Slant column MAX-DOAS measurements of nitrogen dioxide, formaldehyde, glyoxal and oxygen dimer in the urban environment of Athens. Atmos. Environ. 135, 118–131. https://doi.org/10.1016/j.atmosenv.2016.03.048.

Guenther, A., Geron, C., Pierce, T., Lamb, B., Harley, P., Fall, R., 2000. Natural emissions of non-methane volatile organic compounds, carbon monoxide, and oxides of nitrogen from North America. Atmos. Environ. 34, 2205–2230. https://doi.org/10.1016/S1352-2310(99)00465-3.

Guo, Y., Wang, S., Zhu, J., Zhang, R., Gao, S., Saiz-Lopez, A., Zhou, B., 2021. Atmospheric formaldehyde, glyoxal and their relations to ozone pollution under low- and high-NOx regimes in summertime Shanghai, China. Atmos. Res. 258, 105635 https://doi.org/10.1016/j.atmosres.2021.105635.

Hersbach, H., Bell, B., Berrisford, P., Biavati, G., Horányi, A., Muñoz Sabater, J., Nicolas, J., Peubey, C., Radu, R., Rozum, I., Schepers, D., Simmons, A., Soci, C., Dee, D., Thépaut, J.-N., 2023a. ERA5 hourly data on single levels from 1940 to present. Copernicus climate Change service (C3S) climate data store (CDS) [WWW document]. ERA5 hour. Data single levels from 1940 to present. Copernicus Clim. Chang. Serv. Clim. Data Store. https://doi.org/10.24381/cds.adbb2d47.

Hönninger, G., von Friedeburg, C., Platt, U., 2004. Multi Axis differential optical absorption spectroscopy (MAX-DOAS). Atmos. Chem. Phys. Discuss. 4, 231–254.

Hoque, H.M.S., Irie, H., Damiani, A., Rawat, P., Naja, M., 2018a. First simultaneous observations of formaldehyde and glyoxal by MAX-DOAS in the Indo-Gangetic Plain region. Inside Solaris 14, 159–164. https://doi.org/10.2151/sola.2018-028.

Hoque, H.M.S.S., Irie, H., Damiani, A., 2018b. First MAX-DOAS observations of formaldehyde and glyoxal in Phimai, Thailand. J. Geophys. Res. Atmos. 123, 9957–9975. https://doi.org/10.1029/2018JD028480.

Javed, Z., Liu, C., Khokhar, M.F., Tan, W., Liu, H., Xing, C., Ji, X., Tanvir, A., Hong, Q., Sandhu, O., Rehman, A., 2019a. Ground-based MAX-DOAS observations of CHOCHO and HCHO in Beijing and baoding, China. Rem. Sens. 11 https://doi.org/10.3390/rs11131524.

Javed, Z., Liu, C., Khokhar, M.F., Xing, C., Tan, W., Subhani, M.A., Rehman, A., Tanvir, A., 2019b. Investigating the impact of Glyoxal retrieval from MAX-DOAS observations during haze and non-haze conditions in Beijing. J. Environ. Sci. 80, 296–305. https://doi.org/10.1016/j.jes.2019.01.008.

Khokhar, M.F., Naveed, S.I., Butt, J.K., Abbas, Z., 2016. Comparative analysis of atmospheric glyoxal column densities retrieved from MAX-DOAS observations in Pakistan and during MAD-CAT field campaign in Mainz, Germany. Atmosphere 7. https://doi.org/10.3390/atmos7050068.

Kleipool, Q., Ludewig, A., Babic, L.a., Bartstra, R., Braak, R., Dierssen, W., Dewitte, P.J., Kenter, P., Landzaat, R., Leloux, J., Loots, E., Meijering, P., Van Der Plas, E., Rozemeijer, N., Schepers, D., Schiavini, D., Smeets, J., Vacanti, G., Vonk, F., Veefkind, P., 2018. Pre-launch Calibration Results of the TROPOMI Payload On-Board the Sentinel-5 Precursor Satellite, Atmospheric Measurement Techniques. https://doi.org/10.5194/amt-11-6439-2018.

Kluge, F., Hüneke, T., Knecht, M., Lichtenstern, M., Rotermund, M., Schlager, H., Schreiner, B., Pfeilsticker, K., 2020. Profiling of formaldehyde, glyoxal, methylglyoxal, and CO over the Amazon: normalized excess mixing ratios and related emission factors in biomass burning plumes. Atmos. Chem. Phys. 20, 12363–12389. https://doi.org/10.5194/acp-20-12363-2020.

Kumar, V., Beirle, S., Dörner, S., Mishra, A.K., Donner, S., Wang, Y., Sinha, V., Wagner, T., 2020. Long-term MAX-DOAS measurements of NO2, HCHO, and aerosols and evaluation of corresponding satellite data products over Mohali in the Indo-Gangetic Plain. Atmos. Chem. Phys. 20, 14183–14235. https://doi.org/10.5194/acp-20-14183-2020.

Kurucz, R.L., Furenlid, I., Brault, J., Testerman, L., 1984. Solar flux atlas from 296 to 1300nm. National Solar Observatory, Sunspot, New Mexico.

Lerot, C., Hendrick, F., Van Roozendael, M., Alvarado, L.M.A., Richter, A., De Smedt, I., Theys, N., Vlietinck, J., Yu, H., Van Gent, J., Stavrakou, T., Müller, J.F., Valks, P., Loyola, D., Irie, H., Kumar, V., Wagner, T., Schreier, S.F., Sinha, V., Wang, T., Wang, P., Retscher, C., 2021. Glyoxal tropospheric column retrievals from TROPOMI -multi-satellite intercomparison and ground-based validation. Atmos. Meas. Tech. https://doi.org/10.5194/amt-14-7775-2021.

Li, X., Brauers, T., Hofzumahaus, A., Lu, K., Li, Y.P., Shao, M., Wagner, T., Wahner, A., 2013. MAX-DOAS measurements of NO2, HCHO and CHOCHO at a rural site in Southern China. Atmos. Chem. Phys. 13, 2133–2151. https://doi.org/10.5194/acp-13-2133-2013.

Liu, Z., Wang, Y., Vrekoussis, M., Richter, A., Wittrock, F., Burrows, J.P., Shao, M., Chang, C.C., Liu, S.C., Wang, H., Chen, C., 2012. Exploring the missing source of glyoxal (CHOCHO) over China. Geophys. Res. Lett. 39, 6–10. https://doi.org/10.1029/2012GL051645.

Ludewig, A., Kleipool, Q., Bartstra, R., Landzaat, R., Leloux, J., Loots, E., Meijering, P., Van Der Plas, E., Rozemeijer, N., Vonk, F., Veefkind, P., 2020. In-flight calibration results of the TROPOMI payload on board the Sentinel-5 Precursor satellite. Atmos. Meas. Tech. 13, 3561–3580. https://doi.org/10.5194/amt-13-3561-2020.

MacDonald, S.M., Oetjen, H., Mahajan, A.S., Whalley, L.K., Edwards, P.M., Heard, D.E., Jones, C.E., Plane, J.M.C., 2012. DOAS measurements of formaldehyde and glyoxal above a south-east Asian tropical rainforest. Atmos. Chem. Phys. 12, 5949–5962. https://doi.org/10.5194/acp-12-5949-2012.

Mahajan, A.S., Prados-Roman, C., Hay, T.D., Lampel, J., Pöhler, D., Großmann, K., Tschritter, J., Frieß, U., Platt, U., Johnston, P., Kreher, K., Wittrock, F., Burrows, J.P., Plane, J.M.C., Saiz-Lopez, A., 2014. Glyoxal observations in the global marine boundary layer. J. Geophys. Res. Atmos. 119, 6160–6169. https://doi.org/10.1002/2013JD021388.

Mali, P., Biswas, M.S., Steffen, B., Thomas, W., Hulswar, S., Inamdar, S., Mahajan, A.S., n. d.. Aerosol measurements over India: comparison of MAX-DOAS measurements with ground-based (AERONET) and satellite-based (MODIS) data. Aerosol Air Qual. Res.

Meller, R., Moortgat, G.K., 2000. Temperature dependence of the absorption cross sections of formaldehyde between 223 and 323 K in the wavelength range 225-375 nm. J. Geophys. Res. 105, 7089–7101.

Myriokefalitakis, S., Vrekoussis, M., Tsigaridis, K., Wittrock, F., Richter, A., Brühl, C., Volkamer, R., Burrows, J.P., Kanakidou, M., 2008. The influence of natural and anthropogenic secondary sources on the glyoxal global distribution. Atmos. Chem. Phys. 8, 4965–4981. https://doi.org/10.5194/acp-8-4965-2008.

Office of the Registrar General, 2011. Office of the Registrar General & Census Commissioner, India [WWW Document]. Minist. Home Aff. Gov. India. URL. https://censusindia.gov.in/2011-Common/CensusData2011.html.

Ortega, I., Berg, L.K., Ferrare, R.A., Hair, J.W., Hostetler, C.A., Volkamer, R., 2016. Elevated aerosol layers modify the O2-O2 absorption measured by ground-based MAX-DOAS. J. Quant. Spectrosc. Radiat. Transf. 176, 34–49. https://doi.org/10.1016/j.jqsrt.2016.02.021.

Peters, E., Wittrock, F., Großmann, K., Frieß, U., Richter, a., Burrows, J.P., 2012. Formaldehyde and nitrogen dioxide over the remote western Pacific Ocean: SCIAMACHY and GOME-2 validation using ship-based MAX-DOAS observations. Atmos. Chem. Phys. 12, 11179–11197. https://doi.org/10.5194/acp-12-11179-2012.

Plane, J.M.C., Saiz-Lopez, A., 2006. UV-visible differential optical absorption spectroscopy (DOAS). In: Heard, D.E. (Ed.), Analytical Techniques for Atmospheric Measurement. Wiley-Blackwell, Oxford, UK, pp. 147–188.

Platt, U., Stutz, J., 2008. Differential Optical Absorption Spectroscopy - Principle and Applications. https://doi.org/10.1007/978-3-540-75776-4.

Rossignol, S., Aregahegn, K.Z., Tinel, L., Fine, L., Nozière, B., George, C., 2014. Glyoxal induced atmospheric photosensitized chemistry leading to organic aerosol growth. Environ. Sci. Technol. 48, 3218–3227. https://doi.org/10.1021/es405581g.

Rothman, L.S., Gordon, I.E., Barber, R.J., Dothe, H., Gamache, R.R., Goldman, A., Perevalov, V.I., Tashkun, S.A., Tennyson, J., 2010. HITEMP, the high-temperature molecular spectroscopic database. J. Quant. Spectrosc. Radiat. Transf. 111, 2139–2150. https://doi.org/10.1016/j.jqsrt.2010.05.001.

Ryan, R.G., Rhodes, S., Tully, M., Schofield, R., 2020. Surface ozone exceedances in Melbourne, Australia are shown to be under NOx control, as demonstrated using formaldehyde:NO2 and glyoxal:formaldehyde ratios. Sci. Total Environ. 749, 141460 https://doi.org/10.1016/j.scitotenv.2020.141460.

Schnell, J.L., Naik, V., W Horowitz, L., Paulot, F., Mao, J., Ginoux, P., Zhao, M., Ram, K., 2018. Exploring the relationship between surface PM2.5 and meteorology in Northern India. Atmos. Chem. Phys. 18, 10157–10175. https://doi.org/10.5194/acp-18-10157-2018.

Schreier, S.F., Richter, A., Peters, E., Ostendorf, M., Schmalwieser, A.W., Weihs, P., Burrows, J.P., 2020. Dual ground-based MAX-DOAS observations in Vienna, Austria: evaluation of horizontal and temporal NO2, HCHO, and CHOCHO distributions and comparison with independent data sets. Atmos. Environ. X 5, 100059. https://doi.org/10.1016/j.aeaoa.2019.100059.

Schreier, S.F., Richter, A., Wittrock, F., Burrows, J.P., 2015. Estimates of free-tropospheric NO2 and HCHO mixing ratios derived from high-altitude mountain

MAX-DOAS observations in the mid-latitudes and tropics. Atmos. Chem. Phys. 15, 31781–31821. https://doi.org/10.5194/acpd-15-31781-2015.
Schweitzer, F., Magi, L., Mirabel, P., George, C., 1998. Uptake rate measurements of methanesulfonic acid and glyoxal by aqueous droplets. J. Phys. Chem. A 102, 593–600. https://doi.org/10.1021/jp972451k.
Seinfeld, J.H., Pandis, S.N., 2016. Atmospheric Chemistry and Physics: from Air Pollution to Climate Change. John Wiley & Sons, New York, New York.
Serdyuchenko, A., Gorshelev, V., Weber, M., Chehade, W., Burrows, J.P., 2014. High spectral resolution ozone absorption cross-sections – Part 2: temperature dependence. Atmos. Meas. Tech. 7, 625–636. https://doi.org/10.5194/amt-7-625-2014.
Setokuchi, O., 2011. Trajectory calculations of OH radical- and Cl atom-initiated reaction of glyoxal: atmospheric chemistry of the HC(O)CO radical. Phys. Chem. Chem. Phys. 13, 6296–6304. https://doi.org/10.1039/c0cp01942a.
Singh, A., Rastogi, N., Sharma, D., Singh, D., 2015. Inter and Intra-Annual variability in aerosol characteristics over northwestern Indo-Gangetic Plain. Aerosol Air Qual. Res. 15, 376–386. https://doi.org/10.4209/aaqr.2014.04.0080.
Sinreich, R., Volkamer, R., Filsinger, F., Frieß, U., Kern, C., Platt, U., Sebastián, O., Wagner, T., 2007. MAX-DOAS detection of glyoxal during ICARTT 2004. Atmos. Chem. Phys. 7, 1293–1303. https://doi.org/10.5194/acp-7-1293-2007.
Stutz, J., Kim, E.S., Platt, U., Bruno, P., Perrino, C., Febo, A., 2000. UV-visible absorption cross sections of nitrous acid. J. Geophys. Res. 105, 14585–14592.
Tadić, J., Moortgat, G.K., Wirtz, K., 2006. Photolysis of glyoxal in air. J. Photochem. Photobiol. Chem. https://doi.org/10.1016/j.jphotochem.2005.10.010.
Thalman, R., Volkamer, R.A., 2013. Temperature Dependent Absorption Cross-Sections of O2-O2 collision pairs between 340 and 630 nm and at atmospherically relevant pressure. Phys. Chem. Chem. Phys. 15, 15371–15381. https://doi.org/10.1039/C3CP50968K.
Tiwari, Suresh, Hopke, P.K., Pipal, A.S., Srivastava, A.K., Bisht, D.S., Tiwari, Shani, Singh, A.K., Soni, V.K., Attri, S.D., 2015. Intra-urban variability of particulate matter (PM2.5 and PM10) and its relationship with optical properties of aerosols over Delhi, India. Atmos. Res. 166, 223–232. https://doi.org/10.1016/j.atmosres.2015.07.007.
Vandaele, A.C., Hermans, C., Simon, P.C., Carleer, M., Colin, R., Fally, S., Merienne, M.F., Jenouvrier, A., Coquartii, B., 1998. Measurements of the NO2 absorption cross-section from 42000 cm-1 to 10000 cm-1 (238-1000 nm) at 220 K and 294 K. J. Quant. Spectrosc. Radiat. Transf. 59, 171–184.
Volkamer, R., Molina, L.T., Molina, M.J., Shirley, T., Brune, W.H., 2005a. DOAS measurement of glyoxal as an indicator for fast VOC chemistry in urban air. Geophys. Res. Lett. 32, 1–4. https://doi.org/10.1029/2005GL022616.
Volkamer, R., San Martini, F., Molina, L.T., Salcedo, D., Jimenez, J.L., Molina, M.J., 2007. A missing sink for gas-phase glyoxal in Mexico City: Formation of secondary organic aerosol. Geophys. Res. Lett. 34, L19807 https://doi.org/10.1029/2007GL030752.
Volkamer, R., Spietz, P., Burrows, J., Platt, U., 2005b. High-resolution absorption cross-section of glyoxal in the UV-vis and IR spectral ranges. J. Photochem. Photobiol. Chem. 172, 35–46. https://doi.org/10.1016/j.jphotochem.2004.11.011.
Vrekoussis, M., Wittrock, F., Richter, A., Burrows, J.P., 2009. Temporal and spatial variability of glyoxal as observed from space. Atmos. Chem. Phys. 9, 4485. https://doi.org/10.1039/b906300e.
Wagner, T., Beirle, S., Benavent, N., Bösch, T., Lok Chan, K., Donner, S., Dörner, S., Fayt, C., Frieß, U., García-Nieto, D., Gielen, C., González-Bartolome, D., Gomez, L., Hendrick, F., Henzing, B., Li Jin, J., Lampel, J., Ma, J., Mies, K., Navarro, M., Peters, E., Pinardi, G., Puentedura, O., Pukite, J., Remmers, J., Richter, A., Saiz-Lopez, A., Shaiganfar, R., Sihler, H., Van Roozendael, M., Wang, Y., Yela, M., 2019. Is a scaling factor required to obtain closure between measured and modelled atmospheric O4 absorptions? An assessment of uncertainties of measurements and radiative transfer simulations for 2 selected days during the MAD-CAT campaign. Atmos. Meas. Tech. 12, 2745–2817. https://doi.org/10.5194/amt-12-2745-2019.
Wagner, T., Ibrahim, O., Shaiganfar, R., Platt, U., 2010. Mobile MAX-DOAS observations of tropospheric trace gases. Atmos. Meas. Tech. 3, 129–140. https://doi.org/10.5194/amt-3-129-2010.
Washenfelder, R.A., Young, C.J., Brown, S.S., Angevine, W.M., Atlas, E.L., Blake, D.R., Bon, D.M., Cubison, M.J., Gouw, J.A. De, Dusanter, S., Flynn, J., Gilman, J.B., Graus, M., Griffith, S., Grossberg, N., Hayes, P.L., Jimenez, J.L., Kuster, W.C., Lefer, B.L., Pollack, I.B., Ryerson, T.B., Stark, H., Stevens, P.S., Trainer, M.K., 2011. The glyoxal budget and its contribution to organic aerosol for Los Angeles , California. during CalNex 116, 1–17. https://doi.org/10.1029/2011JD016314, 2010.
Wennberg, P.O., Bates, K.H., Crounse, J.D., Dodson, L.G., McVay, R.C., Mertens, L.A., Nguyen, T.B., Praske, E., Schwantes, R.H., Smarte, M.D., St Clair, J.M., Teng, A.P., Zhang, X., Seinfeld, J.H., 2018. Gas-Phase reactions of isoprene and its major oxidation products. Chem. Rev. 118, 3337–3390. https://doi.org/10.1021/acs.chemrev.7b00439.
WHO, 2016. Global Urban Ambient Air Pollution Database.
Wittrock, F., Richter, A., Oetjen, H., Burrows, J.P., Kanakidou, M., Myriokefalitakis, S., Volkamer, R., Beirle, S., Platt, U., Wagner, T., 2006. Simultaneous global observations of glyoxal and formaldehyde from space. Geophys. Res. Lett. 33, L16804 https://doi.org/10.1029/2006GL026310.
Xing, C., Liu, C., Hu, Q., Fu, Q., Lin, H., Wang, S., Su, W., Wang, W., Javed, Z., Liu, J., 2020. Identifying the wintertime sources of volatile organic compounds (VOCs) from MAX-DOAS measured formaldehyde and glyoxal in Chongqing, southwest China. Sci. Total Environ. 715, 136258 https://doi.org/10.1016/j.scitotenv.2019.136258.
Zhang, S., Wang, S., Zhang, R., Guo, Y., Yan, Y., Ding, Z., Zhou, B., 2021. Investigating the sources of formaldehyde and corresponding photochemical indications at a suburb site in Shanghai from MAX-DOAS measurements. J. Geophys. Res. Atmos. 126, e2020JD033351 https://doi.org/10.1029/2020JD033351.